

2023

Chondrocyte mitochondrial dynamics during differentiation in mineralization

<https://hdl.handle.net/2144/48170>

"Downloaded from OpenBU. Boston University's institutional repository."

BOSTON UNIVERSITY

ARAM V. CHOBANIAN & EDWARD AVEDISIAN SCHOOL OF MEDICINE

Thesis

**CHONDROCYTE MITOCHONDRIAL DYNAMICS DURING DIFFERENTIATION
IN MINERALIZATION**

by

DERRICK EKANAYAKE

B.S., University of Notre Dame, 2021

Submitted in partial fulfillment of the
requirements for the degree of
Master of Science

2023

Approved by

First Reader

Louis C. Gerstenfeld, Ph.D.
Professor of Orthopaedic Surgery

Second Reader

Beth Bragdon, Ph.D.
Professor of Orthopaedic Surgery

ACKNOWLEDGMENTS

I would like to thank Dr. G, Dr, B, and Dr. Kirber for their help and continued support.

CHONDROCYTE MITOCHONDRIAL DYNAMICS DURING DIFFERENTIATION IN MINERALIZATION

DERRICK EKANAYAKE

ABSTRACT

Background/Objective: Converging evidence in recent years suggests growth chondrocytes, involved in the integral process of endochondral bone formation and fracture healing, exhibit a dynamic bioenergetic profile despite residing in the nutrient poor cartilaginous environment. Specifically, chondrocytes show an increased dependence on mitochondrial derived oxidative phosphorylation during differentiating, collagen product, but to a differing extent when mineralizing.

Therefore, quantitative analysis of mitochondrial dynamics during these varying processes serves to corroborate existing metabolic studies and further elucidate the role of oxidative metabolism during the endochondral process.

Methods: The murine chondroprogenitor cell line ATDC5 was used, and groups were cultured in differentiating, collagen promoted, and mineralizing conditions. Fluorescence confocal 3D image acquisition and bioimaging analysis was used to quantify changes in mitochondrial volume and branch length per mitochondria along with organization and colocalization changes of the actin cytoskeleton to mitochondria in the various conditions over 21 days.

Results: We showed that chondrocyte differentiation resulted in significantly increased mitochondrial volume and fusion when compared to non-differentiating groups, and in collagen promoted groups, mitochondrial volume was significantly

higher. Additionally, we showed that the process of mineralization resulted in a significant decrease in mitochondrial volume and branch length per mitochondria by day 21 of the experiment. Finally, colocalization analyses of the actin cytoskeleton to mitochondria showed significantly increased overlap in non-differentiating cells when compared to differentiating conditions.

Conclusions: These findings suggest that collagen production is likely an energetically taxing process and mineralization does not heavily rely on oxidative metabolism. Furthermore, the actin cytoskeleton likely plays a role in mitochondrial remodeling that coincides with mitochondrial fission and fusion; increased fission is associated with actin accumulation to mitochondria and fusion is associated with actin disassociation from the outer mitochondrial membrane.

TABLE OF CONTENTS

| | |
|--|-----|
| ACKNOWLEDGMENTS | iv |
| ABSTRACT | v |
| TABLE OF CONTENTS | vii |
| LIST OF TABLES | ix |
| LIST OF FIGURES | x |
| LIST OF ABBREVIATIONS | xi |
| INTRODUCTION | 1 |
| CHONDROCYTE METABOLISM | 2 |
| CHONDROCYTE MITOCHONDRIA | 4 |
| CHONDROCYTE DIFFERENTIATION | 6 |
| Role of Ascorbic Acid in Chondrocyte Differentiation | 8 |
| MATRIX MINERALIZATION | 10 |
| TERMINAL CELL FATE | 12 |
| Mitochondrial Morphology in Apoptotic Cell Death | 14 |
| ACTIN CYTOSKELETON AND CHONDROCYTE DIFFERENTIATION | 16 |
| A Link Between the Actin Cytoskeleton and Mitochondrial Dynamics | 17 |
| SPECIFIC AIMS | 19 |
| METHODS | 20 |
| CELL MODEL | 20 |
| IMMUNOFLUORESCENCE | 21 |
| CELL IMAGING | 22 |

| | |
|---|----|
| IMAGE ANALYSIS..... | 22 |
| STATISTICAL ANALYSIS..... | 24 |
| RESULTS..... | 25 |
| MITOCHONDRIAL VOLUME..... | 25 |
| BRANCH LENGTH PER MITOCHONDRIA..... | 29 |
| ACTIN CYTOSKELETON ORGANIZATION..... | 32 |
| Actin Parallelness, Density, and Bundling..... | 33 |
| ACTIN TO MITOCHONDRIA COLOCALIZATION..... | 35 |
| DISCUSSION..... | 39 |
| AA INCREASES MITOCHONDRIAL VOLUME WHEN DIFFERENTIATING..... | 39 |
| ACTIN CYTOSKELETON AND MITOCHONDRIAL DYNAMICS..... | 41 |
| MITOCHONDRIAL FRAGMENTATION AND MINERALIZATION..... | 43 |
| LIMITATIONS AND FUTURE WORK..... | 46 |
| CONCLUSION..... | 48 |
| REFERENCES..... | 49 |
| CURRICULUM VITAE..... | 58 |

LIST OF TABLES

| | |
|-------------------------------------|----|
| Table 1. Cell Media Conditions..... | 21 |
|-------------------------------------|----|

LIST OF FIGURES

| | |
|---|----|
| Figure 1. Relationship of Bax-Drp1 and Mitochondrial Fragmentation | 16 |
| Figure 2. Relationship of Actin Colocalization to Mitochondrial Morphology..... | 18 |
| Figure 3. Morphological Changes in Mitochondria..... | 27 |
| Figure 4. Mitochondrial Volume of Cells in Different Media | 28 |
| Figure 5. Branch Length Per Mitochondria of Cells Different Media..... | 31 |
| Figure 6. Actin Staining in Different Media Conditions..... | 32 |
| Figure 7. Actin Cytoskeleton Organization During Different Media Conditions... | 34 |
| Figure 8. Actin and Mitochondria Co-Staining | 36 |
| Figure 9. Actin Concentration in Relation to Mitochondrial Dynamics | 37 |
| Figure 10. Actin Overlap with Mitochondria | 38 |

LIST OF ABBREVIATIONS

| | |
|---------------------|-------------------------------------|
| AA..... | Ascorbate Acid |
| ABP | Actin Binding Protein |
| α -KG | α -Ketoglutarate |
| ALP..... | Alkaline Phosphatase |
| α -MEM..... | α -Modified Eagle Medium |
| ANOVA..... | Analysis of Variance |
| ATDC5..... | ATDC5 Teratoma-derived Cell Line |
| ATP | Adenosine Triphosphate |
| β -GP | β -Glycerol Phosphate |
| BMP..... | Bone Morphogenic Protein |
| CYT-C | Cytochrome C |
| DMEM | Dulbecco's Modified Eagle Medium |
| DRP1..... | Dynamin-related Protein 1 |
| ECM | Extracellular Matrix |
| ETC | Electron Transport Chain |
| F12 | Ham's F12 Nutrient Mixture |
| HIF1 α | Hypoxia Inducible Factor 1 α |
| IMS | Intermembrane Space |
| INF..... | Interferon |
| ITS..... | Insulin-Transferrin-Selenium |
| Mfn1, 2 | Mitofusins 1, 2 |

| | |
|-------------|---|
| MIP | Maximum Intensity Z-projection |
| MOMP | Mitochondrial Outer Membrane Permeabilization |
| MSC | Mesenchymal Stem Cell |
| mtDNA | Mitochondrial DNA |
| MV | Matrix Vesicle |
| OMM..... | Outer Mitochondrial Membrane |
| OPA1 | Optic Atrophy Type 1 |
| PDH..... | Prolyl Hydroxylase |
| RUNX2 | Runt-related Transcription Factor 2 |
| SF..... | Stress Fiber |
| TCA | Tricarboxylic Acid Cycle |
| TET..... | Ten-eleven Translocation |
| TNAP | Tissue-Nonspecific Alkaline Phosphatase |

INTRODUCTION

Bone formation occurs either by intramembranous or endochondral ossification. The latter, responsible for the formation of the appendicular skeleton, occurs through a unique process in which bone tissue is preceded by a hyaline cartilage anlage [1]. Eventual bone deposition, skeletal growth, and post-natal fracture healing are coordinated by the concerted effects of chondrocytes of the growth plate—growth chondrocytes—in proliferation, differentiation, ECM homeostasis, matrix mineralization, and cell death. Despite residing in the nutrient starved cartilaginous environment, early evidence suggesting chondrocytes exclusively utilize glycolytic metabolism becomes further antiquated as recent works report increasing oxidative phosphorylation (OXPHOS) during differentiation and collagen production [2] but to a differing extent when mineralizing [3]. Therefore, the dynamics of mitochondria organelle formation and structure are inextricably linked to the oxidative capacity of cells. These organelles are thought to undergo extensive morphological remodeling, now known to occur via the actin cytoskeleton, that underpin these metabolic shifts [4, 5]. Thus, characterization of mitochondrial dynamics is vital to substantiate previous work and further elucidate the role of OXPHOS in growth chondrocyte bioenergetics.

CHONDROCYTE METABOLISM

The in vivo cartilage environment in which chondrocytes reside and maintain lacks vasculature, nerves, and lymphatics. As a result, chondrocytes receive O_2 and nutrients via diffusion from neighboring elements. In the growth plate, chondrocytes are supplied by capillaries of the epiphyseal artery, underlying metaphyseal artery and perichondral bone and in articular cartilage, chondrocytes are supplied by synovial fluid and the underlying subchondral bone [6]. By virtue of this arrangement, O_2 and nutrient gradients exist across the zonal layers of cartilage tissues. In articular cartilage, O_2 tension has been well documented and reported to range from 2-7%, with the higher levels exhibited in the more superficial layers [7]. A similar glucose gradient lies in the same direction with concentrations below 1mM found in the deeper zone [8]. In endochondral cartilage, however, efforts to measure O_2 and glucose content have produced varying results as the anatomical location inherently presents additional challenges to the acquisition process. Despite this, given growth chondrocytes are known to be functionally more active than those in articular cartilage, nutrient gradients are thought to be more extreme in the growth plate. Because very little O_2 is available in cartilage, chondrocytes have long been thought to heavily rely on glycolytic metabolism for energy, fully converting glucose to lactate in the production of ATP [9]. Indeed, studies have found that primary chondrocytes derive as much as 95% of their ATP from glycolysis and only around 1-10% from oxidative phosphorylation (OXPHOS) [9]. Recent work

comparing superficial and deep cells of articular cartilage, however, suggests deep cells derive a greater proportion of their ATP from OXPHOS due to lower glucose and bolstered O₂ supply from underlying bone, demonstrating that the microenvironmental conditions have an influence on chondrocyte metabolism [8, 10].

Additionally, shifts in glycolytic and OXPHOS utilization also occurs as endochondral differentiation progresses by virtue of distinct cellular processes. For example, during proliferation glycolytic metabolism functions to meet the needs of a rapid production of new cells [9]; the notion of glycolysis in cell proliferation is also seen in cancer cells, highly proliferative cells that exhibit extensive glycolytic metabolism despite the presence of O₂ (Warburg effect). Therefore, increased glycolytic flux could facilitate the production of macromolecules and cellular components integral to proliferation, although an exact understanding still remains to be further developed. Nevertheless, early chondrocytes utilize glycolysis not strictly as a result of the anoxic cartilaginous environment but in order to proliferate, inherently deriving a majority of their ATP through glycolysis [11,12]. In contrast, during differentiation, a process in which cells become more specialized through genetic modulation, growth chondrocytes exhibited an increased dependence on OXPHOS for ATP production [2, 13]. Work by Hollander et al. [13] further supports this as inhibition of OXPHOS via several ETC chain inhibitors precluded chondrogenic differentiation, thereby suggesting differentiation is an energetically taxing process requiring a switch

from glycolysis to OXPHOS. Furthermore, during endochondral differentiation, growth chondrocytes are also engaged in other cellular processes such as ECM synthesis, matrix mineralization, and cell death—vital processes that likely further influence bioenergetic shifts. Indeed, in ATDC5 cells, differentiation under mineralizing conditions was associated with diminished oxidative function and protein production when compared to non-mineralizing conditions [3] and in situ terminally differentiated chondrocytes exhibited a higher degree of uncoupled mitochondria and a near undetectable reliance on OXPHOS prior to cell death [14]. Taken together, accumulating evidence thus suggests chondrocytes exhibit a dynamic metabolic profile, with shifts in glycolysis and OXPHOS as a result of the combined microenvironmental conditions and cellular processes.

CHONDROCYTE MITOCHONDRIA

Mitochondria are dynamic organelles integral to numerous cellular functions. Briefly, these double-membraned organelles house the enzymes for several key oxidative metabolic pathways: the Citric Acid Cycle (TCA) which occurs in the outer matrix; and OXPHOS, which occurs along proteins embedded in the inner mitochondrial membrane. Additionally, mitochondria also regulate the oxidation status of the cell, mediate programmed apoptotic cell death, and participate in intracellular calcium handling [reviewed in 15]. In chondrocytes, mitochondria only take up 1-2% of the cellular volume compared to 15-20% in other cell types, are often fragmented or missing proteins integral to the electron

transport chain [7], and exhibit relatively low oxygen consumption rates [10]. Still, even in chondrocytes, it has long been established that mitochondria are inextricably linked to the bioenergetic status of the cell as dynamic morphological changes occur in response to environmental and metabolic stress [3]. Therefore, dynamic remodeling of mitochondria is a tightly orchestrated process that occurs through fission and fusion events, which are separate functions that serve different purposes and are uniquely carried out by guanosine triphosphatases (GTPases) in the dynamin family [3]. In the fission process, fission machinery, namely Drp1, is recruited from the cytosol to distinct fission sites at the outer mitochondrial membrane (OMM). Fusion occurs similarly, with recruitment of fusion machinery to fusion sites on mitochondria where GTPases Mfn1, Mfn2 mediate fusion of the OMM and Opa1 the inner mitochondrial membrane. In cells, fusion functions to counteract environmental stress and starvation through mitochondrial complementation, a process in which fusing with other mitochondria rescues or enhances the ability of the organelles and in abundance, increases the overall mitochondrial capacity of the cell [18, 19]. For example, damaged mitochondria can fuse with healthy mitochondria wherein the function of the damaged mitochondria is rescued through sharing of mtDNA, proteins, lipids, and additional intracellular contents and in times of energetic demand, fusion mediates the sharing of proteins and lipids that bolster the OXPHOS capacity of the cell [18]. Fission, the morphologically opposite process, occurs in the presence of excess nutrients, widespread cellular dysfunction, and healthy

mitophagy [16]. Generally, the extent of fission or fusion do not match, and so two ultrastructural characterizations of the mitochondrial network arise: fragmented when mitochondria have predominantly undergone fission; and elongated when extensive/majority fusion has occurred. Interestingly, both fission and fusion are integral to the differentiation process as knockout of fusion/fission proteins inhibited cellular differentiation [16, 20]. Specifically, fission necessary for mitochondrial biogenesis and sufficient mitochondrial content in daughter cells [16] and fusion, for its previously mentioned role in bolstering cellular OXPHOS capacity [21]. However, increased mitochondrial biogenesis, a process connected to fission, was also seen to contribute to the increased OXPHOS capacity of osteogenic cells during differentiation [22]. Therefore, ultrastructural changes in mitochondrial architecture during differentiation are complex as studies report both fusion and fission during chondrogenic differentiation [20-22].

CHONDROCYTE DIFFERENTIATION

Chondrogenic differentiation is a highly orchestrated and temporally specific process modulated by the presence and induction of various signaling proteins, transcription factors, and ECM elements. In the growth plate, chondrocytes are organized into characteristic zones of-proliferation, differentiation, mineralization, cell death, and ossification that is indicative of their distinct cell function and state. During early fetal development, bone formation is initiated by condensation of MSCs (mesenchymal stem cells). Subsequent

activity of SOX9 initiates chondrogenic differentiation of cells at the interior of the condensate to become proliferative chondrocytes [1, 23]. After initial proliferation, marrow invasion occurs with the establishment of primary and secondary ossification centers which establish the overall bone model of the developing skeletal element. During subsequent growth there is rapid proliferative activity of chondrocytes at the growth plate that both increases the size of the cartilage matrix and aids in driving longitudinal bone growth. Proliferative chondrocytes predominantly produce type 2 collagen and high levels of aggrecan, are flatter and arranged close together, and have collagens arranged parallel to the articular surface of long bone [24].

In the transitional zone, postmitotic chondrocytes, also called pre-hypertrophic chondrocytes, begin to differentiate into swollen cells. Runx2 along with numerous BMPs are responsible for initiating hypertrophic differentiation and completion to a terminally differentiated state [1, 23]. Together, these proteins facilitate the distinct changes that characterize the hypertrophic phenotype: rounding of cell shape; increased expression of type X collagen and lower aggrecan [25]; and increased alkaline phosphatase (ALP) activity [1,23]. In conjunction with proliferative cells, increasing cell size during hypertrophy drives longitudinal growth of the skeletal element. As cell move more proximal to the chondro-osseus border, they become terminally differentiated. Visually, they are fewer in quantity, arranged in columns perpendicular to the articular surface, and

synthesize notably larger amounts of collagen than that seen in the proliferative zone, albeit at lesser amounts [24].

Role of Ascorbic Acid in Chondrocyte Differentiation

In most mammals, including humans, endogenous production of Ascorbate Acid (AA) is not possible due to the absence of the enzyme gluconolactone oxidase. Therefore, sufficient dietary intake of AA, also known as Vitamin C, is essential; humans deficient in AA develop excessive skin bruising and gum bleeding known as scurvy. In cells, apart from its protective properties as a potent antioxidant, AA functions in numerous regulatory capacities that link it to a variety of cellular dynamics. In perhaps its most well-known role, AA is a cofactor for the $\text{Fe}^{2+}/\alpha\text{-KG}/\text{O}_2$ dependent prolyl hydroxylases (PDHs) [26] responsible for the hydroxylation of proline residues of procollagen chains in the ER. Therefore, because the hydroxylation status of collagen governs secretion and deposition into the ECM, AA serves a crucial role in ECM/collagen homeostasis [26]. Furthermore, AA mediated PDH hydroxylation also functions in what Shapiro et al. [27] call the O_2 sensing capability of chondrocytes, a protein system that connects cellular metabolism and environmental O_2 via alterations in the hydroxylation status of HIF1 α . Briefly, in normoxic conditions, PDH hydroxylation of HIF1 α proline residues destabilize the transcription factor, promoting its degradation and absence of downstream effects. However, under hypoxic conditions, O_2 dependent PDH hydroxylation does not occur and HIF1 α stabilization initiates downstream effects that promote anaerobic glycolysis and

inhibit OXPHOS in two notable ways: (1) activation of pyruvate dehydrogenase kinase inhibits pyruvate flux into the mitochondria Citric Acid Cycle (TCA); (2) translocation of HIF1 α into the nucleus upregulates transcription of glycolytic enzymes. Thus, HIF1 α controls glucose utilization in response to hypoxic conditions, generating increased glycolytic ATP and inhibiting mitochondrial activity to lower the O₂ needs of cells [26, 27]—linking AA, in at least one way, to cellular metabolism. Indeed, in MSC cultures, AA treatment in normoxic environments enhanced cell expansion via increased OXPHOS, a result of elevated HIF1 α breakdown and unperturbed mitochondrial activity [28]. Additionally, in BMP2-induced chondrogenic differentiation of murine C3H10T $\frac{1}{2}$ cells, AA treatment increased protein accumulation, oxidative capacity, and ATP production [2]. Furthermore, AA is also extensively used in cell culture models to promote both chondrogenic and osteogenic differentiation as numerous studies reported the presence of hypertrophic markers—increased Runx2, collagen type X, and ALP activity—with addition of AA [29, 30] and significantly less chondrogenic expression in its absence [31]. In murine chondroprogenitor ATDC5 cells, AA was shown to shorten chondrogenic proliferation periods [32] and induce early onset of the differentiated phenotype [33], suggesting a temporally advantageous application of AA when studying chondrogenic differentiation in in-vitro settings. However, the exact mechanism of AA induced differentiation is still unclear—specifically, if AA mediated gene expression is dependent on collagen synthesis given ECM signaling is known to govern

cellular dynamics. Studies have shown that implantation into an AA-conditioned ECM was enough to induce hypertrophy via integrin signaling and collagen inhibition abrogated expression of the hypertrophic phenotype [32, 33]. However, contrasting findings by Sullivan et al. [34] suggested that AA-induced gene expression is independent of collagen synthesis, as inhibition of collagen hydroxylation in AA-treated cells still resulted in hypertrophic expression and implantation of immature cells in AA-conditioned ECM was not enough to induce differentiation. Although further work is required to fully elucidate the exact mechanism of AA mediated differentiation, new evidence suggests AA may assert its affects through DNA histone modification; AA is also a cofactor for TET enzymes responsible for cytosine demethylation. Interestingly, knockout studies of various TET's enzymes have reported impeded and abnormal proliferation, differentiation, and stemness of a wide range of STEM cells and their progeny [26, 35].

MATRIX MINERALIZATION

As cells hypertrophy and terminally differentiate, matrix mineralization occurs in the surrounding ECM. Notable microenvironmental changes include: MM13 expression, a metalloproteinase that degrades aggrecan and collagenous fibers; and less collagen production by terminal cells under mineralizing conditions [1, 23]. In the ECM, mineralization occurs from the continuous deposition of calcium-phosphate crystals, hydroxyapatite, into the collagen

scaffolding [36]. Although extracellular levels of phosphate and calcium are two determinants for mineralization, the occurrence of mineralization is more dependent on systemic levels of phosphate, a potent molecular species also implicated in fracture healing, hypertrophic cell death, and growth plate maturation [36, 37, 38]. Furthermore, the source of phosphate has also been shown to be of significance; studies altering the P_i source reported detectable mineral-crystal formation only when cells were treated with β -GP (beta glycerol phosphate) despite exogenous supplementation of P_i [13]. Therefore, it is thought that ALP, an ectoenzyme tethered to the outer surface of hypertrophic cells, is integral to mediating matrix mineralization. Through its hydrolyzation of phosphodiester bonds of extracellular species, ALP does two things: (1) liberates free P_i from phosphodiester bond containing species such as β -GP for incorporation into growing aggregates; (2) hydroxylates the phosphodiester bond in PP_i , an inhibitor of mineralization, diminishing its tonic inhibition. Therefore, it is thought that ALP serves in the mineralization process not only to increase extracellular P_i but perhaps more importantly to reduce extracellular PP_i inhibition, altering the P_i/PP_i ratio in such a way that calcium-phosphate aggregation and subsequent mineralization is promoted [36, 39].

Additionally, matrix vesicles (MVs) in the ECM, equipped with membrane associated tissue nonspecific alkaline phosphatase (TNAP) and annexin V, are also known to facilitate mineralization in a process called MV-associated mineralization [39, 40]. Akin to ALP, high TNAP activity at the exterior of MVs

facilitates the hydrolytic cleavage of inorganic phosphate. However, instead of nucleation in the ECM, P_i moves into MVs via phosphate channels as a result of the increased local concentration [39]. In addition, intracellular P_i is further increased through the activity of several intra-vesicular enzymes that liberate P_i from phospholipids of the inner leaflet membrane of MVs [36, 39]. Ca^{2+} flux into MVs is thought to be modulated by annexin V interaction with ECM elements, namely collagen X and 2 [41]. Binding of collagen to these calcium dependent channel causes Ca^{2+} influx and accumulation in MVs. Together, as the intra-vesicular concentration of P_i and Ca^{2+} increases, progressive nucleation, and eventual eruption out of MVs leads to deposition of hydroxyapatite crystals into the collagen scaffolding. Further support to the theory of MV-associated mineralization was established by the seminal work of Boone et al. [42] in identifying calcium phosphate aggregates in both extracellular and intracellular vesicles. As a result, culminating work suggests progression of an intra-vesicular amorphous calcium phosphate to the crystalline structure in extracellular vesicles originates at dysfunctional, calcium-phosphate rich mitochondria, in which removal and trafficking to the ECM occurs via mitophagy and sequential vesicle budding [43].

TERMINAL CELL FATE

As terminal hypertrophic cells near the chondro-osseous border, increase expression of MM9 promotes angiogenesis and programmed cell death; osteoid,

secreted from osteogenic cells, is then laid down in continuation of the existing mineralized matrix and ultimately forms bone [1, 23]. Before this, however, the process of terminal cell death is integral, although the complete loss of cells in this area severely impacts the mechanical integrity of bone [44]. Therefore, terminal cells are thought to meet one of two fates: trans-differentiation or cell death [1]. Although the process of trans-differentiation was initially controversial, studies have found expression of type 1 collagen in MSC and chondrocyte cell culture systems suggesting that trans-differentiation or further differentiation to osteoblast-like cells does occur [25, 45].

The other fate, cell death of terminal cells, has been evidenced by the presence of membrane blebbing and diminished cell size in lacunae adjacent to the chondro-osseous junction. Efforts to understand the mechanism(s) of terminal cell death have pointed to apoptosis as characteristic chromatin condensing, DNA fragmentation, and cellular blebbing from proteolysis was observed [45]. In apoptosis, programmed proteolytic cell degradation is thus known to occur through an intrinsic or extrinsic pathway that both converge on the downstream activation of cytosolic caspases, proteolytic enzymes [46]. Specific to the intrinsic pathway, however, is the crucial process of mitochondrial outer membrane permeabilization (MOMP) in mediating caspase activation; pore formation facilitates release of mitochondrial intermembrane space (IMS) proteins into the cytosol, like cytochrome c (cyt-c), and their subsequent activation of caspase enzymes. Interestingly, in terminal cells of the growth plate,

cyt-c and caspase-3 were reported to be increased prior to MOMP [47], and mitochondria exhibited a maturation-dependent loss of membrane potential and oxidative capacity [14], thereby indicating terminal cells are primed for cell death via apoptosis. Dynamic control of the OMM permeabilization status is predominantly governed by the Bcl-2 family of proteins, of which two subclasses exist: anti-apoptotic proteins such as Bcl-2; and pro-apoptotic proteins such as Bax. Present in both the cytosol and the OMM, changes in localization of the two classes to the OMM co-ordinate cell life and fate. Although Bax is constitutively expressed, early stages of apoptosis have been shown to coincide with increased Bax translocation to OMM foci [48]. Temporal accumulation during apoptosis thus leads to MOMP, release of cyt-c, and activation of the caspase cascade. In the growth plate, Bax was seen to be increased in mitochondria of mature cells while Bcl-2 was only localized to mitochondria of immature cells [47]. Thus, a decrease in Bcl-2/Bax ratio in terminal cells is indicative of apoptotic cell death.

Mitochondrial Morphology in Apoptotic Cell Death

Although the occurrence of mitochondrial fragmentation has been reported in several non-apoptotic cellular events, fragmentation is invariably associated with apoptosis [49]. In some worm species, fission events have been seen early in apoptosis, leading some to believe mitochondrial fission functions in an integral step of the early apoptotic pathway [50]. Substantiation to this is given by findings that show in cells treated with STS, an agent that induces apoptosis, Bax

focal accumulation at the OMM occurs at distinct fission sites where Drp1 colocalizes with Bax [51]. Although a great deal of nuance surrounds the exact mechanism, Bax mediated MOMP early in apoptosis is thought to not only facilitate cyt-c release, but also the translocation of IMS protein DDP/TIMM8a to the cytosol [52]. Once in the cytosol, DDP/TIMM8a recruits Drp1 to the OMM, promoting colocalization with Bax that then further stimulates Bax recruitment and oligomerization to the OMM. [49, 50, 52]. Completion of Bax recruitment to the OMM was shown to correlate with apoptotic mitochondrial fission and lower mitochondrial volume [48]. Although additional work into the temporal interdependence of Bax-Drp1 co-recruitment, cyt-c release, and apoptotic mitochondrial fragmentation remains crucial, numerous studies have well established the necessity of both Bax and Drp1 function in apoptotic mitochondrial fission [48-51]. Cells expressing a dominant negative inhibitor of Drp1 exhibited delayed or complete inhibition of mitochondrial fragmentation, cytochrome c release, and cell death and apoptosis-induced fragmentation was not observed in cells expressing a Bax mutant. Furthermore, despite initial Bax translocation occurring irrespective of Drp1 function, temporal Bax coalescence was significantly less, did not correlate with changes in gross mitochondrial morphology, and apoptosis did not occur in cells missing Drp1 function (Figure 1). Taken together, converging evidence suggests that colocalization of Bax and Drp1 is crucial to a mechanistic role of mitochondrial fragmentation in the early apoptotic pathway.

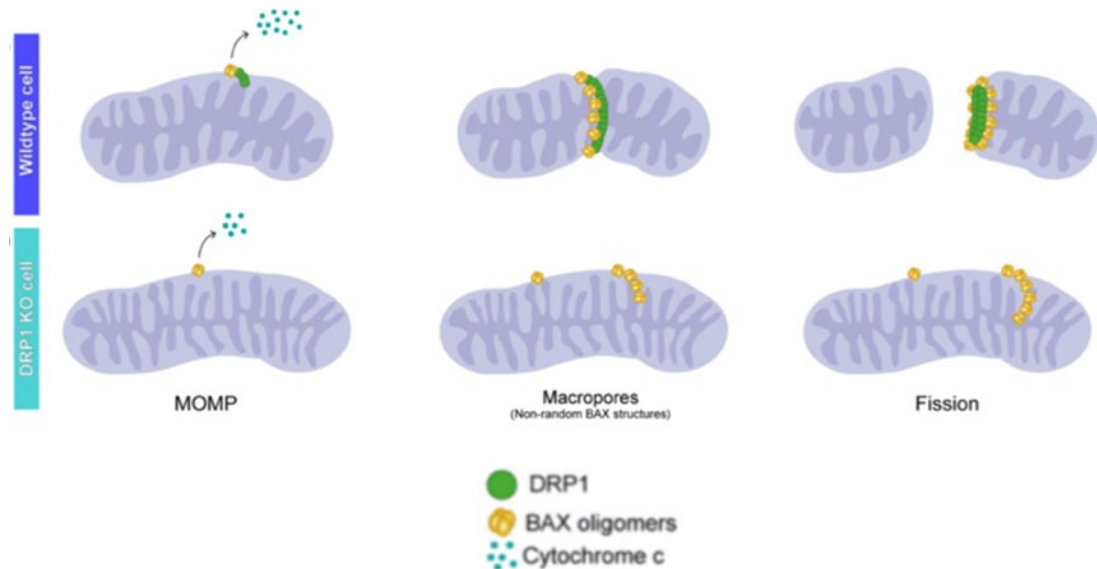


Figure 1. Relationship of Bax-Drp1 and Mitochondrial Fragmentation. WT cells show Bax oligomerization, cyt-c release, and apoptotic mitochondrial fragmentation due to Drp1 function. In Drp1 KO cells, cyt-c release and downstream apoptosis is accompanied by aberrant Bax accumulation and the absence of mitochondrial fission. (Adapted from Maes, et al. 2019)

ACTIN CYTOSKELETON AND CHONDROCYTE DIFFERENTIATION

In addition to cell-cell signaling and cell-matrix interactions, accumulating evidence also implicates the actin cytoskeleton as a mediator of phenotypical changes during chondrogenic differentiation [4, 53]. In cells, actin exists in two forms: a globular monomeric form (G-actin) and a filamentous form (F-actin) composed of two helically coiled actin multimeric units. F-actin filaments are polarized with a fast-growing end (plus or barbed) and a slow growing end (minus or pointed) in which incorporation and dissociation of G-actin occurs in an ATP dependent manner [54]. Further assembly of actin filaments into bundles known as stress fibers (SF) also occurs; numerous types of SF exist, endowing cells with essential properties such as structural integrity and cellular movement

[54]. Regulation of F-Actin polymerization, assembly, and organization is a product of the integrated effects of numerous Rho-family GTPases and their associated downstream actin-binding proteins (ABP). Together, various Rho-family modules influence actin dynamics through severing, capping, nucleating, and/or elongating filaments [4, 54]. For example, chondrogenic differentiation is an integrated result of RhoA/ROCK proliferative effects antagonized by Rac1/Cdc42 hypertrophic effects [55]. In addition, changes in ABP dynamics have also been implicated in the differentiation process; increased expression of adersin in hypertrophic cells was shown to reorganize the actin cytoskeleton, induce hypertrophic gene expression, and alter cell size and shape towards the differentiated phenotype [56]. Therefore, organizational changes of the actin cytoskeleton are indicative of the differentiation status of cells, however, the relationship of the actin cytoskeleton in differentiating chondrocytes remains to be well characterized.

A Link Between the Actin Cytoskeleton and Mitochondrial Dynamics

Converging evidence in recent years also points to actin as a major mediator of mitochondrial remodeling. Although several mechanisms have been proposed, pioneering evidence has centered around the necessity of Mitochondrial Endoplasmic Reticulum Contacts (MERC) as initiation sites of fission [5,57]. Specifically, ER-anchored formin INF2 interacts with OMM-located formin activating Spire1C, leading to actin polymerization into foci at the OMM. However, recent evidence also suggests that actin recruitment to the

mitochondrial surface occurs independent of MERC formation and accumulates in a non-focal arrangement [58]. Regardless, the force of actin polymerization is thought to play an essential role in pre-constricting bulky mitochondria as Drp1 alone is not large enough to fully cut mitochondria, thereby suggesting a necessity of actin in the fission process. Subsequent colocalization of cytosolic Drp1 to actin foci, oligomerization into a ring structure spanning the OMM, and GTP hydrolysis leads to ultimate mitochondrial scission. Understanding of mitochondrial fusion was evidenced by removal of actin polymerizing proteins and concomitant elongation of mitochondria [57-59]. Therefore, mitochondrial network formation is associated with actin disassociation from the OMM which critically re-exposes Mfn1/2 and reinstates their fusion activity. Figure 2 depicts the fission/fusion status of mitochondria in relation to actin localization. Although critical evidence continues to shine light on the numerous proteins and mechanisms that govern mitochondrial dynamics, overwhelming evidence indiscriminately points to a role of actin in mediating mitochondrial remodeling.

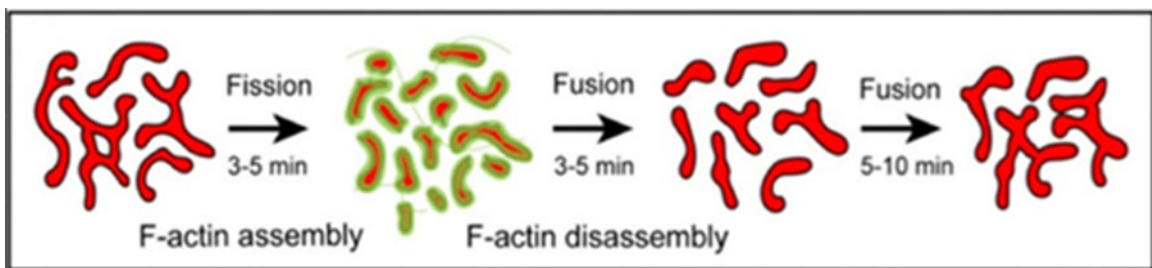


Figure 2. Relationship of Actin Colocalization to Mitochondrial Morphology. The appearance of fragmented mitochondria occurs in relation to actin accumulation around mitochondria and fusion occurs in the absence of actin at the OMM. (From Moore, et al. 2018)

SPECIFIC AIMS

Recent studies report growth chondrocytes exhibit increased oxidative capacity during the processes of differentiation and collagen production and to differing extent during mineralization. While these studies utilize extensive metabolic assays regarding the mitochondrial system, assessment of mitochondrial dynamics and morphology that accompany these finding would further elucidate the role of OXPHOS during vital growth chondrocyte processes.

Therefore, using a robust array of bioimaging analytics, this study aims to quantify changes in mitochondrial dynamics in groups induced to differentiate under varying conditions that promote collagen synthesis and mineralization. These studies further assessed structural relationship of the actin cytoskeleton in mediating the accompanying mitochondrial dynamics during differentiation. Finally, the occurrence of mitochondrial fragmentation and apoptosis during mineralization was examined and the capacity of the fission process to serve in a mechanistic role in the cell death pathway.

METHODS

CELL MODEL

ATDC5 chondroprogenitor cells were expanded in growth medium containing DMEM high glucose F12 1:1 (Life Technologies Inc, Beverley, MA), 5% fetal bovine serum (Life Technologies Inc, Beverley, MA), and 1% penicillin/streptomycin antibiotic (Mediatech Inc, Herndon, VA). After confluence was reached, cells were seeded on 35mm glass bottom FluoroDish™ cell culture plates (World Precision Instruments Inc, Sarasota, FL) at a density of 0.7×10^5 cells per well. After seeding, cells were incubated an additional 2-3 days in the same media composition to reach confluence. Upon 60% confluence, culture medium was changed to Differentiation, Differentiation + AA, and Differentiation + AA + β -GP; untreated cells were left in growth media to serve as control (see Table 1). ATDC5 cell differentiation was induced by supplementation with 5x insulin-transferrin-selenium (Lonza Walkersville Inc, Walkersville, MD). Cell culture medium promoting collagen production was supplemented with 37.5 μ g/ml L-ascorbic Acid (Sigma-Aldrich, St. Louis, MO) and culture medium promoting mineralization was supplemented with 4 mM β -glycerol phosphate (Sigma-Aldrich, St. Louis, MO). The day of first media change was considered Day 0 of differentiation; cells were arrested and permeabilized and stained at Day 7, 14, and 21 post induction. All cells were maintained at 37°C in 5% CO₂ tension for the entire culture period.

Table 1. Cell Media Conditions. All media conditions were supplemented with 5% fetal bovine serum (Life Technologies) and 1% penicillin/streptomycin antibiotic (Mediatech). ¹Life Technologies, ²Lonza BioWhittaker, ³Sigma-Aldrich

| | Medium Name | | | | |
|-----------------------------|-------------------|----------------|--|--|---|
| | Expansion | Growth/Control | Differentiation | Diff + AA | Diff + AA + β -GP |
| Base | DMEM ¹ | | α -MEM ¹ | | |
| Differentiating Supplements | N/A | N/A | 5X insulin-transferrin-selenium ² | | |
| Other Treatment | N/A | N/A | N/A | 37.5 μ g/ml L-Ascorbic Acid ³ | 37.5 μ g/ml L-Ascorbic Acid ³ , 4mM β -glycerol phosphate ³ |

IMMUNOFLUORESCENCE

Staining was done at Day 7, 14, and 21 post induction of differentiation. Prior to each step, ATDC5 cultures were washed three times with prewarmed 1x PBS for 5 minutes (Mediatech Inc, Herndon, VA). A final concentration of 200nM of MitoTracker™ Red CMXRos (Life Technologies Corp, Eugene, OR) in PBS was used to stain cells for 35 minutes at 37°C in 5% CO₂ tension. Cells were fixed with 3.7% formaldehyde for 15 minutes in growth medium and subsequently permeabilized with ice-cold acetone for 5 minutes. Cells were then subject to either cytoskeleton staining or antibody treatment. Actin staining was done at 50 μ g/mL of phalloidin-FITC (Abcam, Branford, CT) at room temperature for 40 minutes in a dark environment. Prior to antibody treatment, cells were blocked in 0.1% BSA in PBS for 10 minutes at room temperature. Cells were then incubated for 30 minutes with anti-Bax (B-9) mouse monoclonal antibody conjugated to

Alexa Fluor® 405 (1:50; Santa Cruz, Dallas, TX) and anti-DRP1 (C-5) mouse monoclonal antibody conjugated to Alexa Fluor® 546 (1:50; Santa Cruz, Dallas, TX). Prolong Gold Antifade reagent with DAPI (Life Technologies Corp, Eugene, OR) was used to stain nuclei and preserve samples.

CELL IMAGING

Image acquisition was done via a Leica SP5 Fluorescence Confocal microscope using a 63X objective oil lens. All images are taken at a resolution of 2048x2048. Single plane images were taken along with Z-stack images at a z-interval of 0.4 μm .

IMAGE ANALYSIS

All image processing was done with NIH FIJI/image software. Image preprocessing was done through FIJI/ImageJ plugin DeconvolutionLab2 [60] and PointSpreadGenerator [61]. When specified, z-sections were used to make Maximal Intensity Projections (MIP). Cellular metrics were analyzed on an individual cell basis or square ROI of $\sim 4000 \mu\text{m}^2$.

Prior to mitochondrial analysis, z-section images of individual cells were cropped and persisting background noise was manually subtracted. Fiji/ImageJ plugin Mitochondria Analyzer [62] was used to assess mitochondrial volume and extent of fusion through branch length per mitochondria. To determine optimal threshold in which mitochondria are selected over image artifacts and noise,

Mitochondria Analyzer feature 'optimize threshold' was used. A block size of 1.25, weighted mean algorithm, and C-value of 10 was determined to create the most accurate segmentation. Mitochondrial volume and branch length per mitochondria of fifty cells cultured in each media condition and time point were analyzed and reported as means.

Quantitative analysis of the actin cytoskeleton arrangement was done in single cells and square ROI of $\sim 4000 \mu\text{m}^2$ using a MIP created from seven z-series image at a z-interval of $0.4 \mu\text{m}$. Cell area was assessed via Set Measurements tool in FIJI/ImageJ. The LPX plugin [63] (filter = lineFilters, linemode = lineExtract) was used to skeletonize MIP at parameters: giwslter = 15, mdnmsLen = 15, pickup = aboveZero, shaveLen = 10, and delLen = 10. Skeletonized images were then masked with binary image and analyzed using LPX plugin (filter = lineFilters, linemode = lineFeature) to assess cytoskeleton parallelness and bundling (skewness of intensity distribution). Cytoskeleton density was measured by dividing i_nPix value output (skeletonized pixel number) by ROI area. Sixteen ROIs from each condition and timepoint were analyzed.

Colocalization analysis was used to assess actin localization to mitochondria in relation to mitochondrial morphology. Pixel-pixel based intensity and object based colocalization methods of MIP created from seven z-series at z-interval of $0.4 \mu\text{m}$ were used. Segmentation using 'moments' for mitochondria in red mitochondria channel and 'Iso_Data' for green actin channel were used to

and fixed ROI of $\sim 4000 \mu\text{m}^2$ was used. FIJI/ImageJ tools Raw Integrated Density, Mean Gray Value, and Integrated Density were used to assess actin concentration (pixel intensity) trend over 21 days. To assess actin colocalization to mitochondria, FIJI/ImageJ function BIOP_JaCoP was used to generate M1 and M2, Mander's split coefficients that represent colocalization of each channel. M1 represents the percentage of red channel that overlaps with green channel and M2 the percentage of green channel overlapping with red. Mander's split coefficients are not overly sensitive to intensity differences between overlaying channels and thus provides a reliable way to assess colocalization via overlap [64]. Fifty ROIs from each condition and timepoint were analyzed.

STATISTICAL ANALYSIS

Two-way Anova was used to compare media conditions and timepoints. Appropriate Post-hoc tests were used following two-way Anova test to determine difference between media conditions and timepoints. All analyses were done at a significance level of $p < 0.05$. All statistical testing and graphing were done through GraphPad Prism.

RESULTS

In the first series of studies, the total mitochondrial content and structure were assessed (Figure 3-5). Figure 3 shows the overall mitochondrial morphology in cells over 21 days cultured in varying conditions. Figure 4 provides quantitative measures of the overall volume of the mitochondrial content while figure 5 assesses the overall branch length of the mitochondrial organelles.

MITOCHONDRIAL VOLUME

Fifty cells from each condition and time point were analyzed and the mean was reported as total volume (Figure 4). ATDC5 cells cultured in non-differentiating media exhibited no significant change in mitochondrial volume between any of the individual times points: day 7 to 14 ($p=0.1726$), 14 to 21 ($p=0.5232$), and 7 to 21 ($p=0.7587$). In comparison cultures grown under both differentiation conditions showed both a significant increase from day 7 to 21 ($p<0.0001$) as well as were significantly higher than non-differentiated cells ($p=0.0003$). ATDC5 cells cultured in differentiation media in the absence of AA (Diff) exhibited significant increases in volume between each of the three time points: day 7 to 14 ($p=0.0089$) and 14 to 21 ($p=0.0365$). Differentiating cells supplemented with ascorbic acid (Diff + AA; 37.5ug/ml) also showed a significant increase in volume from day 7 to 14 ($p=0.0448$) and 14 to 21 ($p<0.0001$), while showing a further significant increase in total mitochondrial volume over those that were not supplemented with AA ($p<0.0001$). In groups supplemented with β -

GP (Diff+AA+ β -GP; 4mM), mitochondrial volume did not change significantly from day 7 to 14 ($p=0.2799$), 14 to 21 ($p=0.7162$) and 7 to 21 ($p=0.0578$). Groups cultured in the absence of β -GP exhibited significant mitochondrial volume increase from day 7 to 14 ($p=0.0190$) and day 14 to 21 ($p=0.0042$); at day 21, mitochondrial volume was significantly higher ($p<0.0001$) in comparison to day 7 of the experiment. Between treatment groups, there was no significant difference in mitochondrial volume at day 7 ($p=0.9466$) and day 14 ($p=0.2491$), however, mitochondrial volume in β -GP treated groups was significantly lower ($p=0.0002$) at day 21.

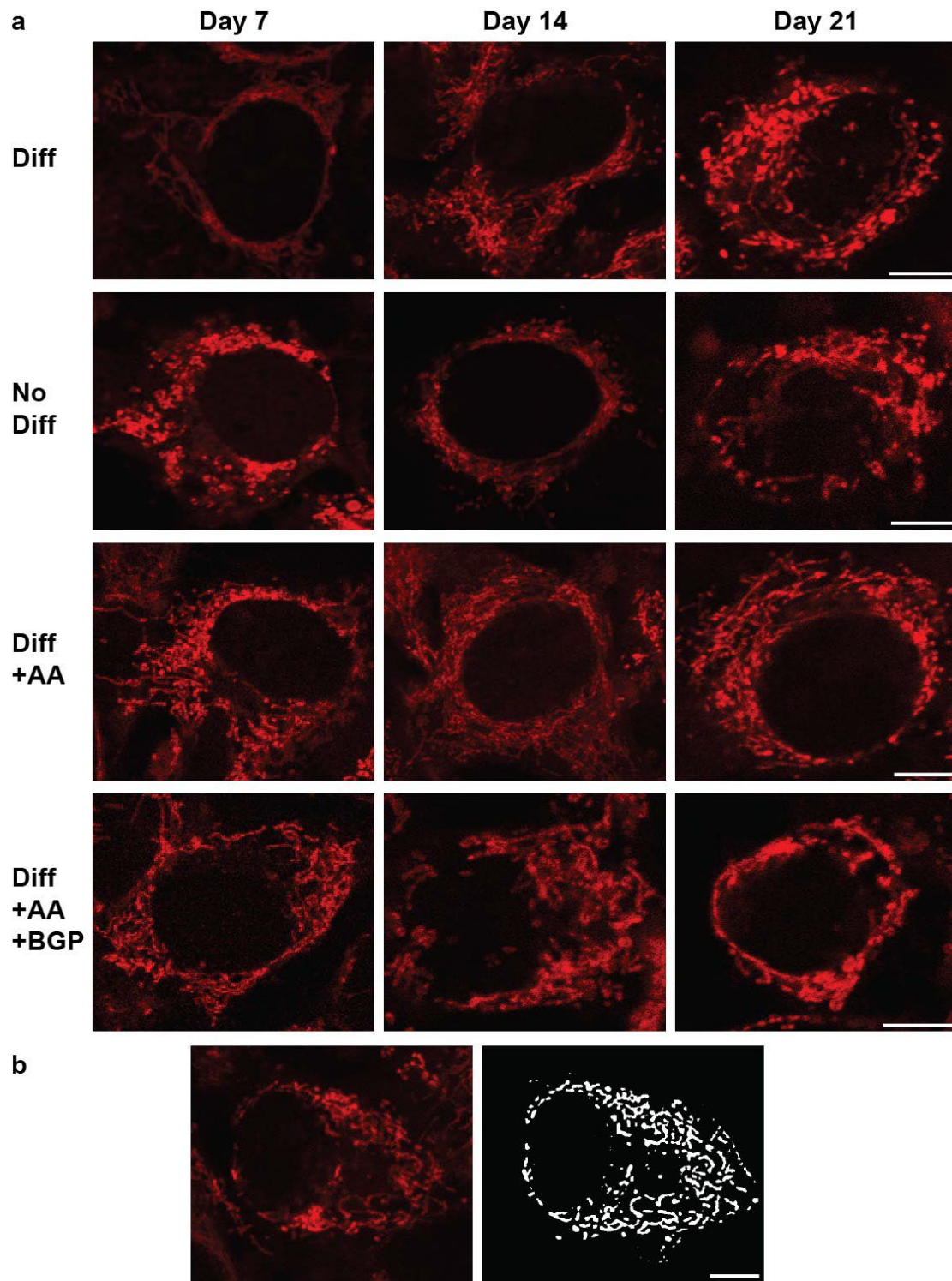


Figure 3. Morphological Changes in Mitochondria. ATDC5 cells (a) under differentiation (Diff), non-differentiating, collagen production (Diff+AA), and mineralization (Diff+AA+BGP) conditions. (b) example of thresholding used for mitochondrial analysis; scale bar 5 μ m

Mitochondrial Volume

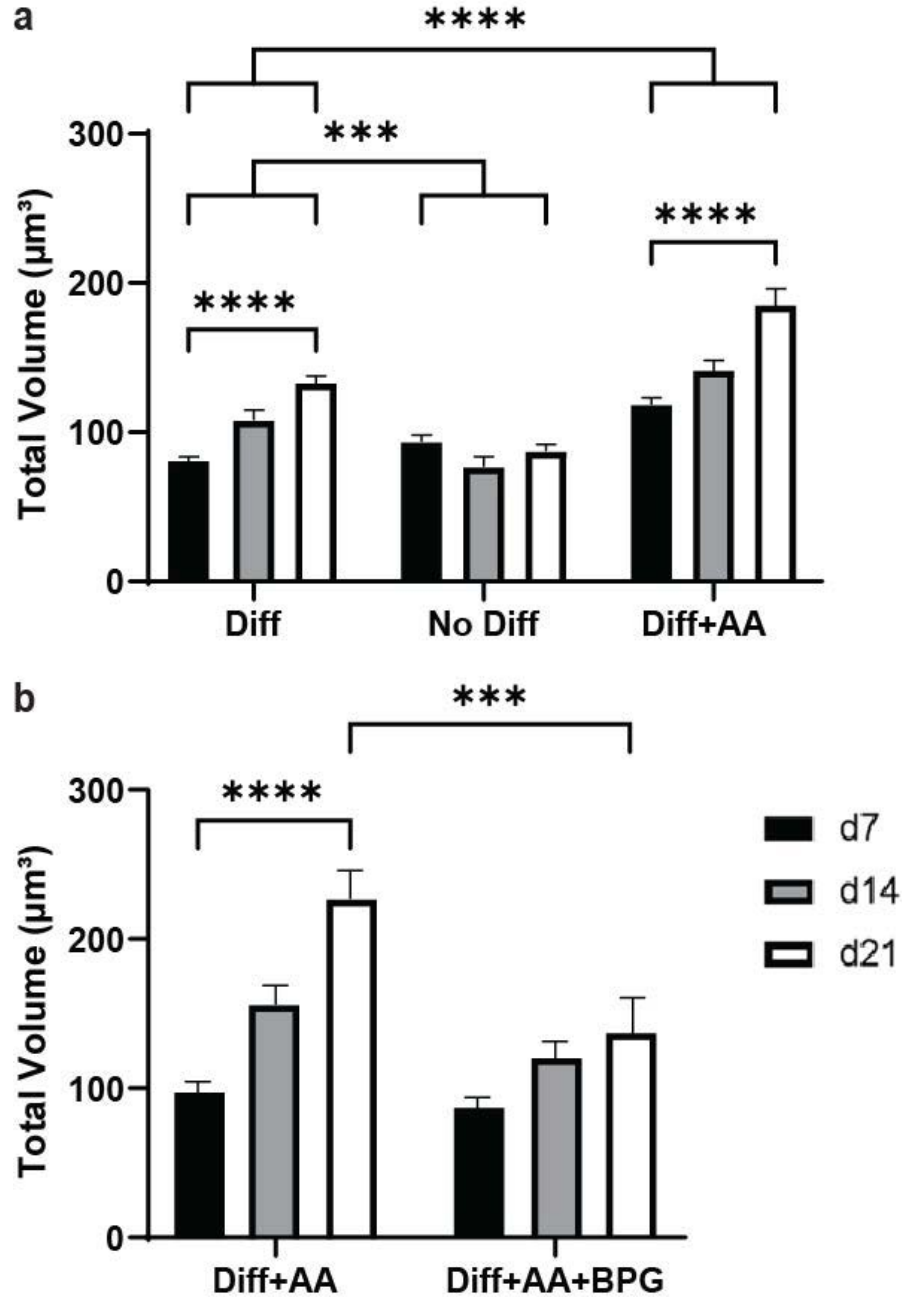


Figure 4. Mitochondrial Volume of Cells in Different Media. (a) Differentiating cells supplemented with AA showed significantly higher mitochondrial volume than those not treated with AA and cells under non-differentiating conditions exhibited significantly lower volume compared to differentiating cells. (b) Compared to non-treated β -GP groups, cells supplemented with β -GP exhibited significantly less mitochondrial volume at day 21. Data represented by means \pm SEM. *** p < 0.001, **** p < 0.0001. $n=50$ cells for each condition at each timepoint

BRANCH LENGTH PER MITOCHONDRIA

The extent of mitochondrial fusion was next assessed based on Branch Length per mitochondria. In this study the sum of all branch lengths in a single cell was divided by the sum of all mitochondria within a cell and reported as branch length per mitochondria (Figure 5). ATDC5 cells cultured in non-differentiating conditions did not show significant change in branch length per mitochondrial between any of the times: day 7 to 14 ($p=0.6874$) and 14 to 21 ($p=0.5109$) nor were there any significant differences over the entire time course of the experiment in non-differentiating conditions: day 7 to 14 ($p=0.57$) day 14 to 21 ($p=0.5$) and day 7 to 21 ($p=0.5$). In contrast, cells cultured in differentiating media exhibited significantly higher branch length per mitochondria between day 7 and 14 ($p=0.0224$) and 14 to 21 ($p<0.0001$). Branch length per mitochondria in cultures further supplemented with AA only showed a significant increase from day 14 to 21 ($p<0.00001$). When comparing differentiating to non-differentiating cells, there was a significant difference in branch length per mitochondria ($p=0.0001$), however, comparison between differentiating groups showed no significant difference in branch length per mitochondria ($p=0.9903$). In groups treated with β -GP, branch length per mitochondria did not exhibit any significant change from day 7 to 14 ($p=0.6592$) and 14 to 21 ($p=0.2334$) but did significantly increases from day 7 to 21 ($p=0.0353$). In groups cultured in the absence of β -GP, branch length per mitochondria did not change significantly from day 7 to 14 ($p=0.1547$), but did increase significantly from day 14 to 21 ($p=0.0076$) and 7 to

21 ($p < 0.0001$). When comparing β -GP treated groups to non-treated groups, there was no significant difference at day 7 ($p = 0.7599$) and 14 ($p = 0.1786$), however, branch length per mitochondria was significantly lower ($p = 0.0039$) in β -GP treated groups at day 21.

Branch Length Per Mitochondria



Figure 5. Branch Length Per Mitochondria of Cells Different Media. (a) Groups induced to differentiate exhibited an increase in branch length per mitochondria from day 7 to 21; non differentiating cells did not exhibit any change. Addition of AA did not increase branch length per mitochondria. (b) Branch length per mitochondria was significantly lower in β -GP treated groups at day 21. Data represented by means \pm SEM. ** $p < 0.01$, *** $p < 0.001$, **** $p < 0.0001$. $n=50$ cells for each condition at each timepoint.

ACTIN CYTOSKELETON ORGANIZATION

Figure 7 shows the actin cytoskeleton organization over 21 days of cell cultured in varying media conditions.

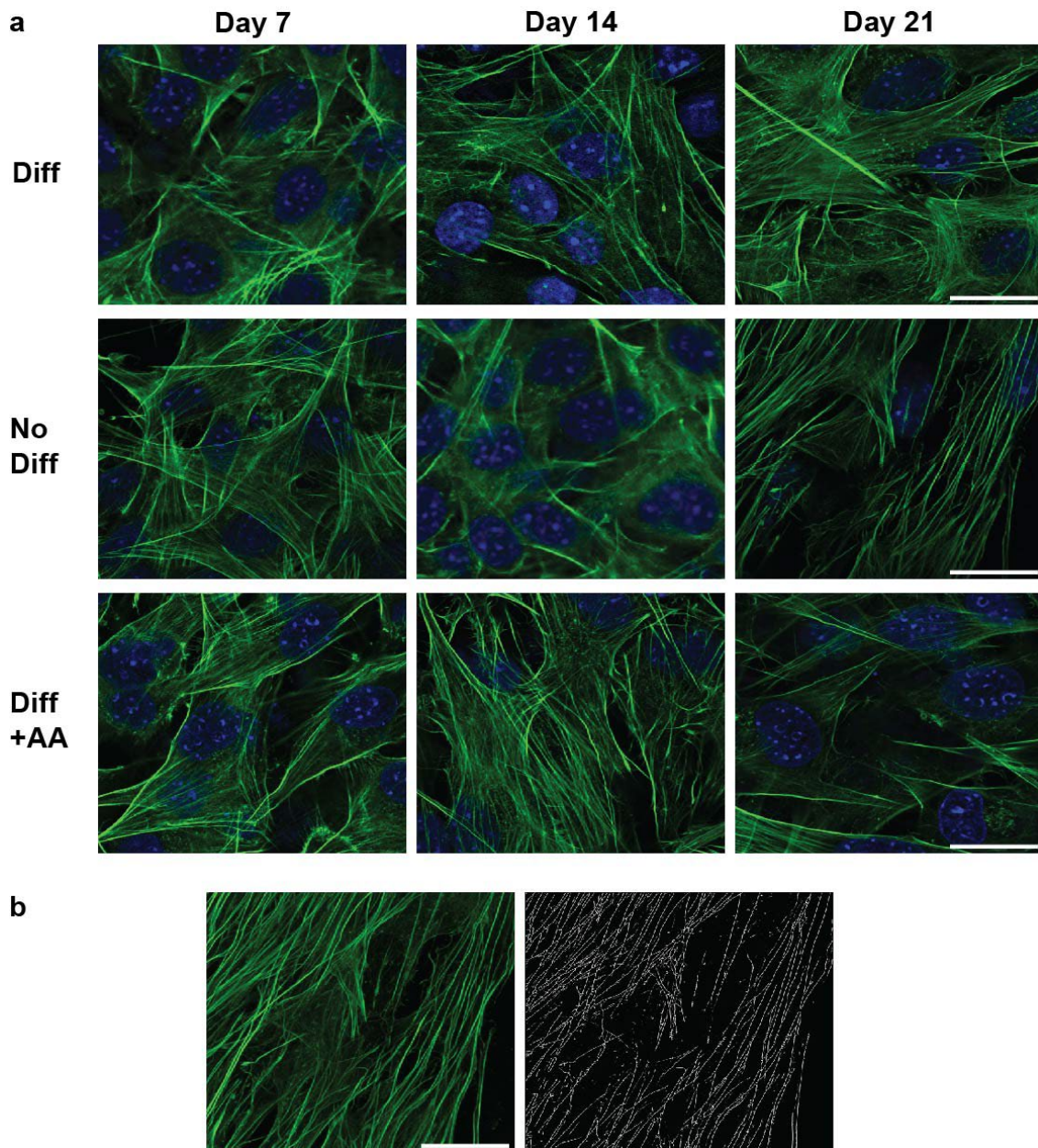


Figure 6. Actin Staining in Different Media Conditions. (a) Confocal images of the actin cytoskeleton in differentiating (Diff), non- differentiating (No Diff), and differentiating conditions supplemented with AA (Diff+AA) at day 7, 14, 21. **(b)** Example MIP skeletonized binarized image used for actin cytoskeleton analysis; scale bar 20 μ m

Actin Parallelness, Density, and Bundling

Analysis of the mean cytoskeleton parallelness, density, and bundling were reported from each timepoint and condition (Figure 7). Given the methodology used by LPX for this analysis, actin cytoskeleton organization was evaluated using a binarized image that allows for quantitative assessment of the organizational arrangement irrespective of potentially confounding pixel intensity values. In all three parameters analyzed, differentiating and differentiating cell supplemented with AA exhibited little change throughout the time course of the experiment. Surprisingly, non-differentiating cell exhibited the most change through the 21 days as the actin cytoskeleton appeared to increase in parallelness and decrease in bundling and organizational density.

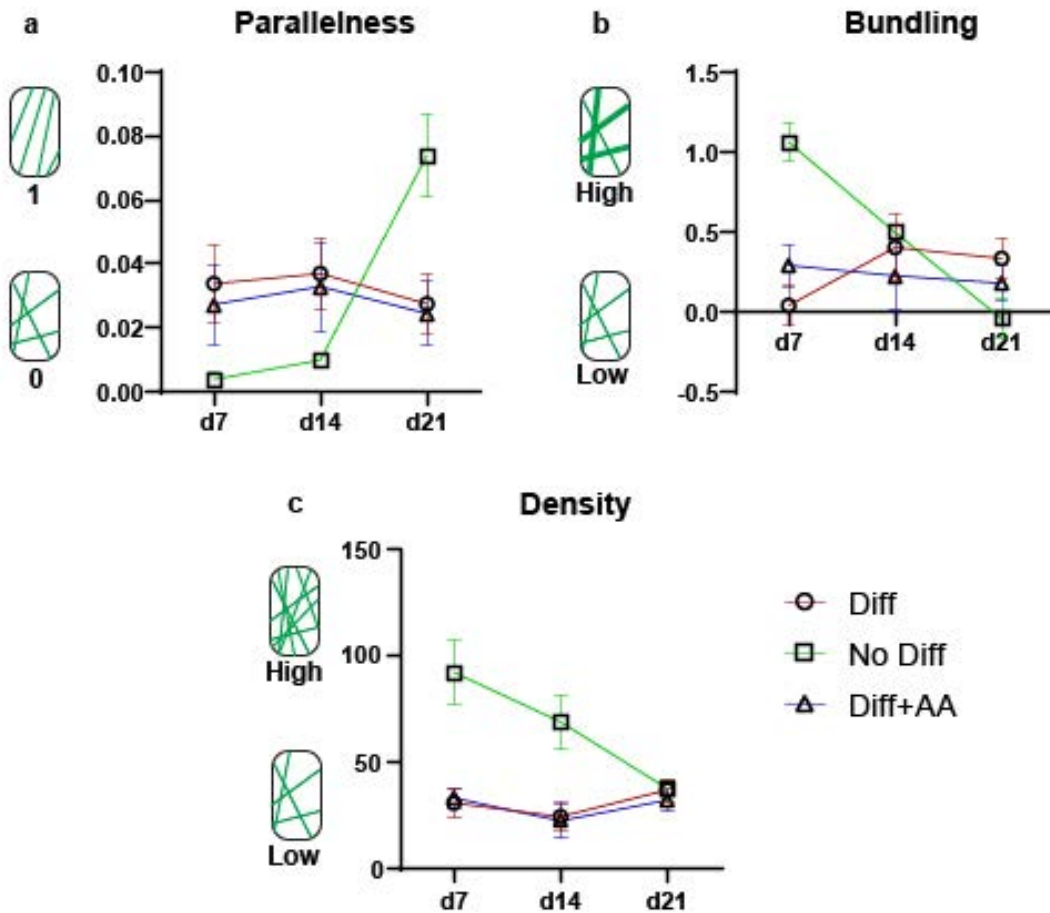


Figure 7. Actin Cytoskeleton Organization During Different Media Conditions. (a)

Parallelness of the actin cytoskeleton in differentiating cells and differentiating cells supplemented with AA did not change over 21 days, however, the actin cytoskeleton appeared to become more parallel in non-differentiating cells. There were no detectable changes in **(b)** bundling of the actin cytoskeleton in both differentiating groups, however, non-differentiating cells exhibited decreased bundling. **(c)** Organizational density did not change in differentiating groups but did decrease in non-differentiating groups. Data represented by mean \pm SEM; n=16 ROIs.

ACTIN TO MITOCHONDRIA COLOCALIZATION

Figure 8 shows cellular mitochondria and actin used to assess the extent of actin colocalization to mitochondria in different media conditions. Actin concentration, reported as actin intensity, was compared against mitochondrial volume and branch length per mitochondria (Figure 9). Interestingly, actin concentration per ROI in all media conditions increased from day 7 to day 21. At the end of 21 days, actin concentration was surprisingly similar in all conditions and exhibited little variance at each time point in all conditions. Mander's split coefficients (M1 and M2) were used to determine the extent of mitochondrial overlap with the cytoskeleton (Figure 10). M1 is indicative of the fraction of total mitochondria in the ROI that overlaps with actin and M2 the total fraction of actin that overlaps with mitochondria. At day 7, comparison between non-differentiating exhibited significantly higher Mander's split coefficients than differentiating cells: M1 $p < 0.0001$ and M2 $p = 0.0001$. Between differentiating groups, there was no significant difference between M1 ($p = 0.1476$) and M2 ($p = 0.5007$) split coefficients. At both day 14 and 21, M1 and M2 coefficients were also significantly higher in non-differentiating cells when compared to differentiating.

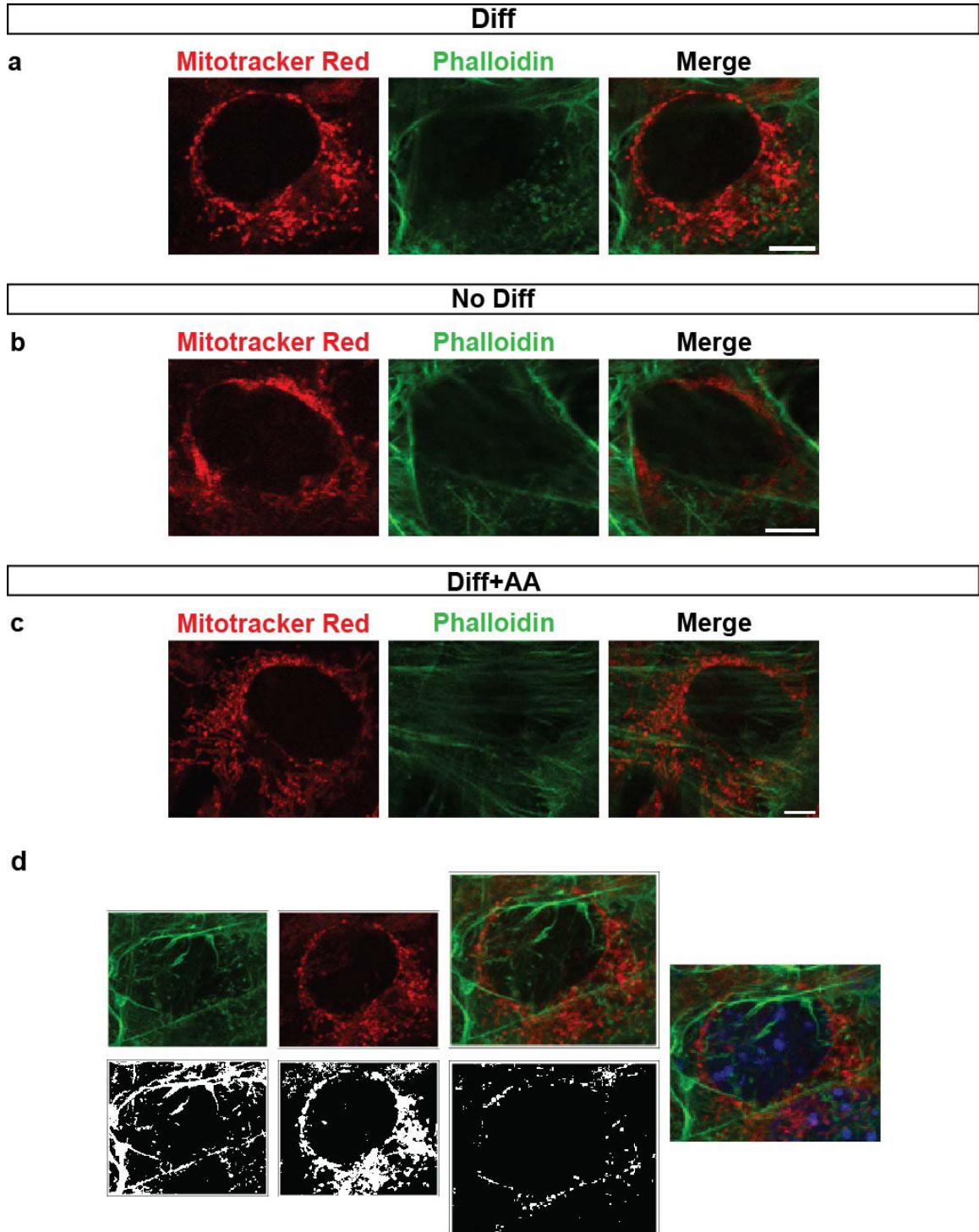


Figure 8. Actin and Mitochondria Co-Staining. (a) Depicts staining at Day 7 of differentiating (Diff), (b) non-differentiating (No Diff), and (c) differentiating cells supplemented with AA (Diff+AA). (d) Example of BIOP_JACoP thresholding analysis; scale bar 5 μ m

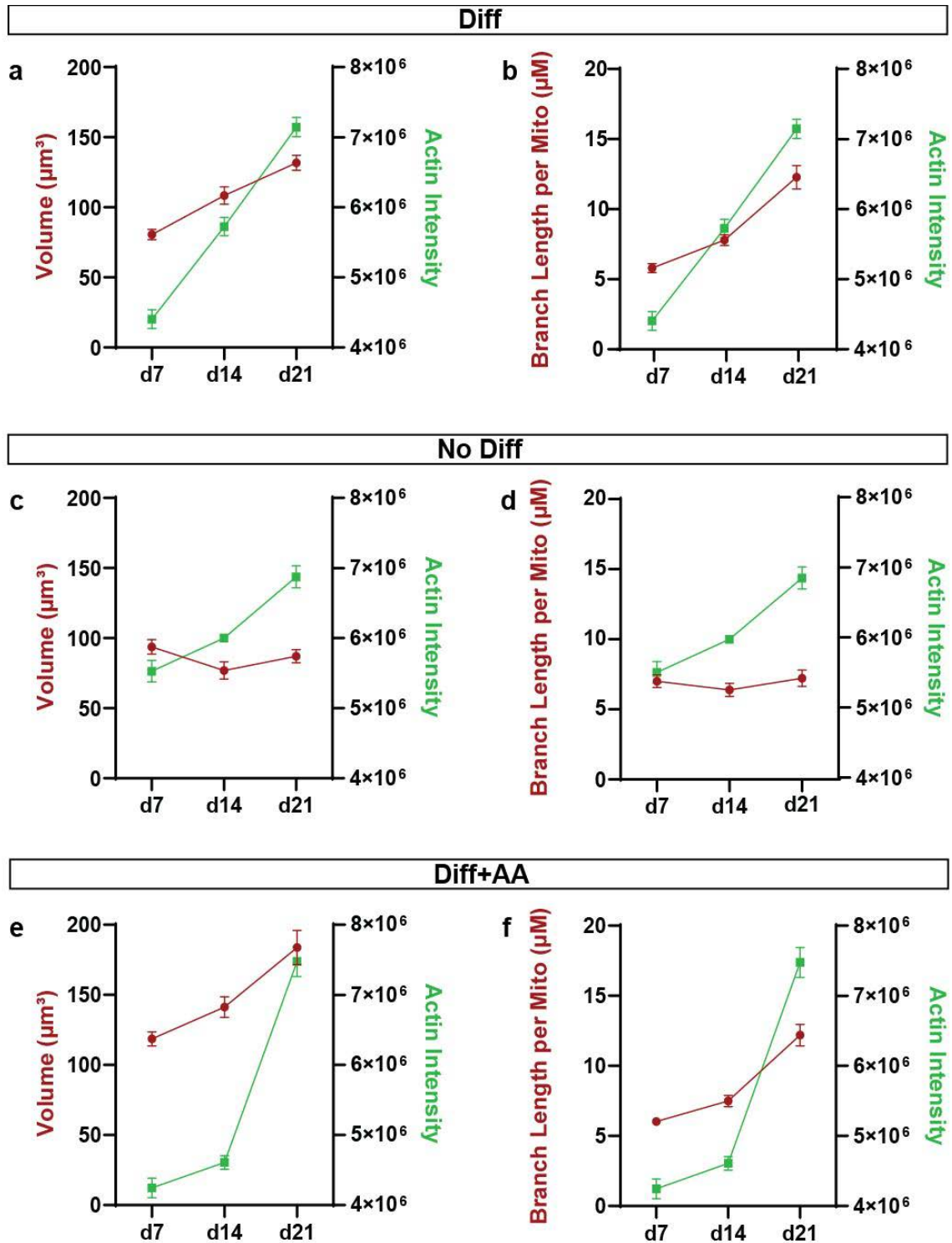


Figure 9. Actin Concentration in Relation to Mitochondrial Dynamics. In both differentiating conditions (a-b, e-f), actin concentration increased with mitochondrial volume and branch length. However, non-differentiating cells (c-d) exhibited increased actin concentration with no changes in volume and branch length per mitochondria. Data represented by means \pm SEM. $n=50$ ROIs.

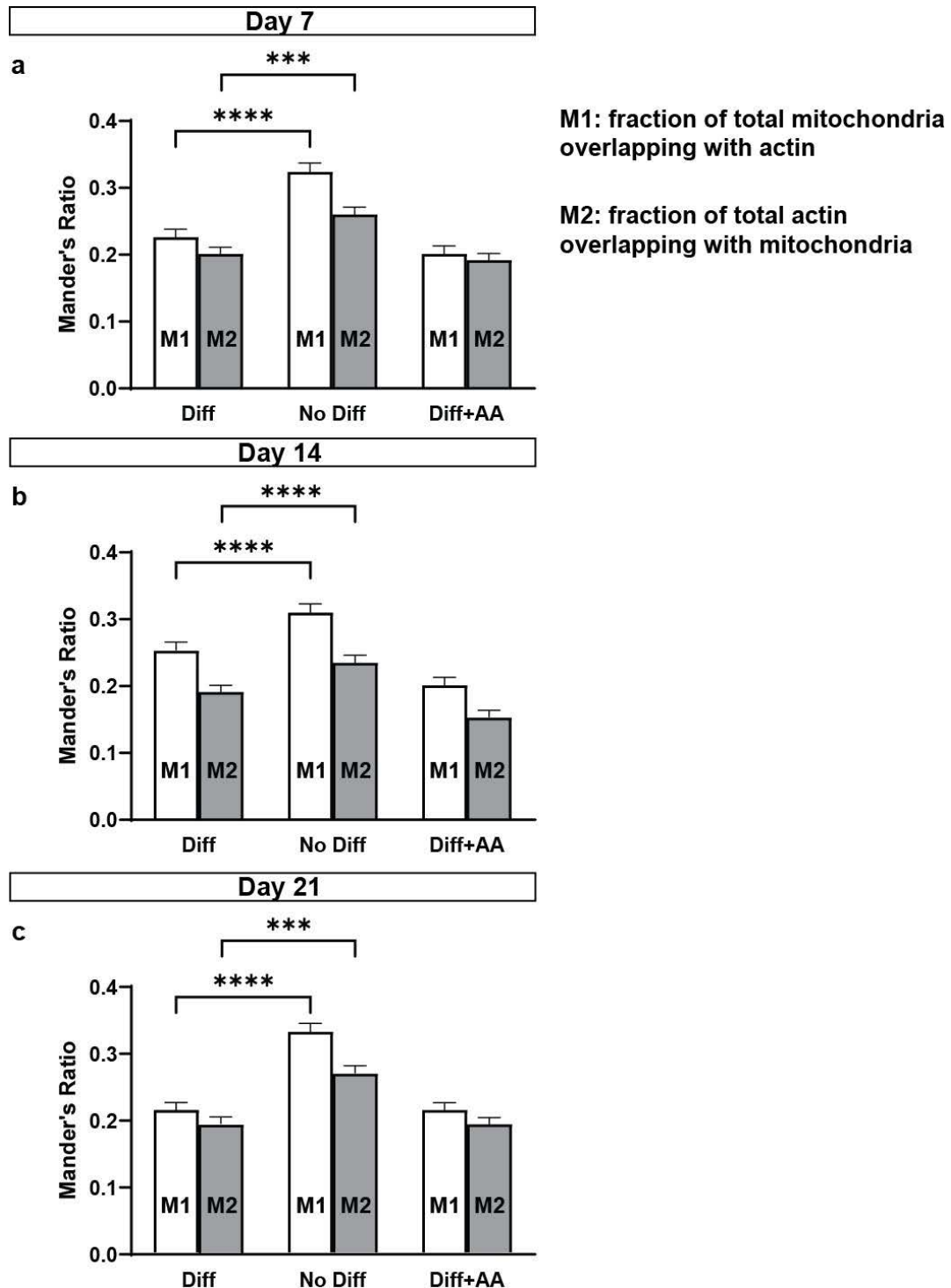


Figure 10. Actin Overlap with Mitochondria. Mander's split coefficients M1 and M2 were used to determine mitochondria overlap with actin and vice versa at (a) day 7, (b) day 14, and (c) day 21. In non-differentiating conditions, the fraction of mitochondria overlapping with actin was significantly higher than both differentiating groups. Data represented by means \pm SEM. *** $p < 0.001$, **** $p < 0.0001$. $n = 50$ ROIs for each condition at each timepoint.

DISCUSSION

Previous metabolic experiments suggest that during differentiation, chondrocytes exhibit an increased reliance on OXPHOS. However, a complete understanding of chondrogenic bioenergetics during the vital process of collagen synthesis and mineralization is lacking--specifically, characterization of mitochondrial dynamics that coincide with shifts in oxidative metabolism during these processes. Thus, in this study, we leveraged quantitative bioimaging approaches to assess structural mitochondrial changes associated both with chondrocyte differentiation, maximal collagen synthesis, and mineralization.

AA INCREASES MITOCHONRIAL VOLUME WHEN DIFFERENTATING

In ATDC5 cells induced to differentiate, we report a significant increase in mitochondrial volume compared to non-differentiating cells over the course of 21 days and a significant increase in mitochondrial volume in AA-treated cells. Although AA treatment in the BMP2-induced differentiation of C3H10T $\frac{1}{2}$ cells increased oxidative function, we cannot necessarily extrapolate these findings to our results and suggest AA-treatment increases OXPHOS as BMP2 likely causes confounding changes to mitochondrial dynamics. Despite this, the increased volume that we report does offer insight into the bioenergetics of collagen production, as a study found increased mitochondrial volume via heightened biogenesis correlates with increased OXPHOS capacity during differentiation of osteogenic cells [22]. Therefore, increased mitochondrial volume as a result of

AA treatment likely serves to bolster the OXPHOS capacity, thereby suggesting collagen production is an energetically taxing process in which chondrocytes rely on mitochondria to meet these energy needs. However, the mechanism in which AA treatment ultimately does this, whether it be through the PDH-HIF1 α system or AA mediated collagen hydroxylation shifting the energetic state and stimulating increased mitochondrial biogenesis and volume is unclear. Given AA has been shown to increase mitochondrial activity through PDH-HIF1 α breakdown, assessment of HIF1 α levels would provide clarifying evidence as a study found downregulation of HIF1 α correlated with increased OXPHOS [4,5]. Regardless, to definitively conclude AA treatment increases OXPHOS and to substantiate our findings regarding increased mitochondrial volume, appropriate metabolic tests demonstrating increased OXPHOS are required.

Although we conclude AA treatment likely increases the oxidative capacity of cells, we would expect this to be accompanied by increased mitochondrial fusion, yet our results showed no significant difference in fusion between differentiating groups. A possible explanation for this could thus be given by the mechanics of mitochondrial biogenesis, a process requiring fission [16]. As a result, the balance between biogenesis via fission and mitochondrial complementation via fusion could co-exist at varying rates, where both collectively increase the oxidative capacity of the cell. Although both are subject to varying factors endowing more or less influence on the overall mitochondrial morphology, our findings of increased volume, indicative of heightened

biogenesis, could dampen the expression of significant fusion between differentiating conditions.

ACTIN CYTOSKELETON AND MITOCHONDRIAL DYNAMICS

Analysis of the organizational status of the actin cytoskeleton under various conditions suggests that during differentiation, actin organization does not exhibit a high degree of variance across 21 days but does surprisingly in non-differentiating cells. Although organizational density, parallelness, and bundling remained at lower degrees in both differentiating groups throughout the time course of the experiment, non-differentiating cells exhibited an increase in parallelness and a large decrease in organizational density and bundling by day 21. Previous studies assessing MSC chondrogenic differentiation report increased SF formation and SF arc, however, we report a decrease in bundling, a parameter indicative of SF formation and qualitatively less actin arcs [52]. We also attempted to quantify the degree of fiber dispersion via actin organizational density, an important distinction as it purely represents the organizational or spatial arrangement of actin fibers irrespective of pixel intensity. However, amongst differentiating groups, this metric did not noticeably change. In addition, we used pixel-intensity based measurements to quantitative actin concentration (actin intensity) to assess changes in the 3D distribution of actin as previous studies report decreasing actin intensity correlates with increasing mitochondrial branch length [36]. Thus, in continuation of this, we expected to see actin

intensity fall from day 7 to 21 in differentiating groups as our findings indicate increasing branch length during this time. However, throughout the 21 days of the experiment, we found actin concentration to increase in both differentiating groups in addition to non-differentiating conditions—a further perplexing finding as our results suggest mitochondria of non-differentiating cells undergo no significant change in branch length and so would likely exhibit an opposite trend than differentiating groups in actin intensity. Given that an increase in actin concentration could be more indicative of other attributes of cell growth and differentiation, a factor not accessed in the aforementioned study, we employed Mander's Split coefficients [64] within the same ROIs to quantitatively assess actin colocalization to mitochondria. Interestingly, we report a significant difference in M1 and M2 split coefficients between differentiating and non-differentiating groups at day 7, 14, and 21. Specifically, M1 and M2 were significantly higher in non-differentiating cells, thereby suggesting a greater fraction of the mitochondrial population overlaps with actin (as assessed by M1) and a greater fraction of the total actin concentration overlaps with mitochondria (as assessed by M2). Taken together, this suggests that despite an increase in actin concentration within all conditions throughout the 21 days, a greater proportion of actin significantly colocalized to mitochondrial in non-differentiating cells and thus could explain the insignificant changes in branch length per mitochondria that we report. Conversely, significantly less mitochondrial overlap with actin in differentiating and AA-treated differentiating cells could then explain

the increased extent of fusion that we report in both media conditions, as less actin colocalization to the OMM allows for sustained exposure of the fusion machinery and increased extent of fusion. It should be noted that although we report no significant difference in M1 and M2 between differentiating and AA-treated cells, supporting our findings that AA treatment did not result in a significant increase in mitochondrial fusion, understanding of the role of the actin cytoskeleton in significantly increasing mitochondrial volume that did parallel AA treatment invites further work. Nevertheless, the significant difference in actin overlap with mitochondria between differentiating and non-differentiating conditions that we report supports the current understanding that actin plays a role in the remodeling of mitochondrial architecture in which colocalization to the OMM facilitates fission and dissociation enables fusion.

MITOCHONDRIAL FRAGMENTATION AND MINERALIZATION

Although we report no significant difference in mitochondrial volume or branch length per mitochondria at day 7 and 14, by day 21 both measurements were significantly lower in ATDC5 cells cultured in mineralizing conditions. Therefore, this significant decline in mitochondrial capacities that would otherwise serve to increase the oxidative capacity of the cell supports previous findings of diminished oxidative metabolism in differentiating cells under mineralizing conditions. Together, this suggests mineralization does not heavily rely on OXPHOS for energy, albeit energy is still necessary as the process of ion

transfer across membranes for nucleation likely requires some degree of energy input. Given the temporal relationship in decreasing mitochondrial dynamics and heightened mineralization and ALP activity [47], mitochondria perhaps function in a non-energetic role during the later stages of mineralization, a notion evidenced by increased calcium-phosphate granules in the inner mitochondrial space of mineralizing cells [42]. Although Ca^{2+} sequestration by mitochondria normally serves to control intracellular calcium levels, the presence of phosphate promotes aggregation and eventual hydroxyapatite deposition. Interestingly, calcium-phosphate accumulation inside mitochondria has been shown to increase with mitochondrial respiration, as electron movement through the phosphorylation sites of the ETC results in a stoichiometric accumulation of calcium and phosphate from the medium, oxidative accumulation of calcium-phosphate has been shown to replace the oxidative phosphorylation of ADP, and inhibition of ATP synthesis from OXPHOS resulted in decreasing inner-mitochondrial granules and discharge into the ECM [65]. Together, although certainly complicated, a possible explanation for the non-significant difference in mitochondrial volume and branch length at the earlier time points could be found within the temporal nature of calcium-phosphate accumulation in mitochondria. Therefore, increasing calcium-phosphate accumulation could result in mitochondrial dysfunction, evidenced by a transition in membrane potential, that tags the aggregate filled mitochondria for mitophagic removal in the early intracellular vesicle pathway of MV-associated mineralization [39, 42, 43]. Thus,

fission, a vital process of mitophagy, and the ultimate fall in mitochondrial volume from removal of aggregate containing mitochondria could provide one explanation for our results in mineralizing cells. Similarly, several studies have also shown a maturation dependent loss of mitochondrial function in terminal cells as they near the endo-osseous border. Specifically, these cells exhibited a transition in mitochondrial membrane potential, a shift from tubular to punctate architecture, and little reliance on OXPHOS in addition to increased Bax accumulation at the OMM [14, 47]. Thus, apoptotic mechanisms are implicated in the mitochondrial dynamics that sensitize these cells towards death; P_i is thought to act as an apoptogen via movement into mitochondria. Therefore, follow up studies characterizing Bax accumulation to OMM and Drp1 relational activity are vital to specifically implicating the fission process in apoptotic cell death during mineralization and better interpreting our results. Interestingly, inhibition of a broad range of caspases have been shown to decrease ALP activity and reduce mineralization, and in ATDC5 cells, inhibition of apoptosis reduced P_i -induced mineralization [14, 38, 47]. Currently, apoptotic fragmentation is thought to possibly function in the release of cyt-c or other IMS proteins, however, newer evidence also suggest fragmentation may directly activate cytosolic caspases [50]. Therefore, because mineralization seems to, in part, be dependent on caspase activity, mitochondrial fragmentation responsible for downstream caspase activity could also be implicated in mineralizing cells and provide

valuable insight into understanding the mechanistic role of apoptotic mitochondrial fragmentation during mineralization.

LIMITATIONS AND FUTURE WORK

Several limitations are present within this study. Due to the heavy reliance on image acquisition, factors such as image background noise, saturation, and microscope settings inherently pose discrepancies and unwanted variance from sample to sample. Although this study implemented the use of several programs designed to combat this, clear image acquisition under normalized conditions is vital for accurate and consistent measurement. Similarly, image analytical methods are also subject to limitations as user bias can be a problem when ascertaining properties of an image by color, shape, pixel intensity, etc. Therefore, automated thresholding and standardized procedures were used in all analyses. However, given the use of individual cell quantifications in some parameters assessed in this study, demarcation of cell boundaries in the x, y, and z directions are inherently subject to some degree of irreducible user bias, despite compromising instance not being used. Additionally, although widely used, colocalization analysis is not indicative of interaction but simply suggests overlap between two proteins and thus conclusions drawn from colocalization analytics can be open to interpretation.

Future work utilizing OCR metabolic studies in AA treated cells along the same experimental procedure is important and would help validate the changes

in mitochondrial dynamics reported in this study in relation to OXPHOS. Additionally, mitochondrial fusion assays in conjunction with image acquisition can be leveraged to better ascertain the extent of fusion in mitochondria, bringing attention to the importance of assay-based studies to validate image analysis and the development of newer protocols that reduce user bias and variance when using image analysis. In continuation of ours and other findings, assessment of the role, if any, of the actin cytoskeleton in mitochondrial biogenesis also serves to provide insightful understanding into the mitochondrial dynamics during various endochondral related functions as we report mitochondrial biogenesis to be a significant mechanism in which chondrocytes increase oxidative capacity.

Given our findings that suggest mitochondrial volume and branch length per mitochondria significantly decreased by day 21, follow up studies characterizing Bax association to mitochondrial and Drp1 colocalization will provide insightful evidence that specifically implicates the increased fragmentation that we report in apoptotic cell death during mineralization.

CONCLUSION

In this study we investigated changes in mitochondrial dynamics that accompany differentiating ATDC5 chondroprogenitor cells under collagen and mineralizing promoted conditions. Crucially, this study serves to corroborate existing metabolic studies that suggest changes in OXPHOS utilization during these process as mitochondrial organelles are intimately linked to oxidative metabolism. In addition to showing increased mitochondrial volume and fusion in differentiating cells compared to non-differentiating cells, we also concluded the collagen production is likely an energy intensive process as increased mitochondrial volume was accompanied. In conjunction with these findings, we were also able to provide evidence of the actin cytoskeleton role in mediating these morphological changes as increased mitochondrial fusion was associated with lower actin colocalization and fission with increased actin colocalization, evidence that is in continuation of current understanding. Finally, this study also found increased fragmentation and loss of mitochondrial volume toward the latter stages of culture periods is when mineralizing and supports the finding of diminished oxidative metabolism of cells during mineralization. Collectively, this works substantiates the emerging significance of mitochondria in growth chondrocyte metabolism and offers valuable insight into metabolic nuances in skeletal growth and the fracture healing process.

REFERENCES

1. Mackie, E. J., Ahmed, Y. A., Tatarczuch, L., Chen, K.-S., & Mirams, M. (2008). Endochondral ossification: How cartilage is converted into bone in the developing skeleton. *The International Journal of Biochemistry & Cell Biology*, *40*(1), 46–62. <https://doi.org/10.1016/j.biocel.2007.06.009>
2. Hussein, A. I., Carroll, D., Bui, M., Wolff, A., Matheny, H., Hogue, B., Lybrand, K., Cooke, M., Bragdon, B., Morgan, E., Demissie, S., & Gerstenfeld, L. (2023). Oxidative metabolism is impaired by phosphate deficiency during fracture healing and is mechanistically related to BMP induced chondrocyte differentiation. *Bone Reports*, *18*, 101657. <https://doi.org/10.1016/j.bonr.2023.101657>
3. Blank, K. C. (2016). *The effect of phosphate availability on chondrocyte metabolic function* (Order No. 10128952). Available from Dissertations & Theses @ Boston University; ProQuest Dissertations & Theses Global: Health & Medicine; ProQuest Dissertations & Theses Global: Science & Technology. (1799278937). <https://ezproxy.bu.edu/login?url=https%3A%2F%2Fwww.proquest.com%2Fdissertations-theses%2Feffect-phosphate-availability-on-chondrocyte%2Fdocview%2F1799278937%2Fse-2%3Faccountid%3D9676>
4. Wai, T., & Langer, T. (2016). Mitochondrial Dynamics and Metabolic Regulation. *Trends in Endocrinology and Metabolism: TEM*, *27*(2), 105–117. <https://doi.org/10.1016/j.tem.2015.12.001>
5. Moore, A. S., & Holzbaur, E. L. F. (2018). Mitochondrial-cytoskeletal interactions: Dynamic associations that facilitate network function and remodeling. *Current Opinion in Physiology*, *3*, 94–100. <https://doi.org/10.1016/j.cophys.2018.03.003>
6. Wirth, T., Syed Ali, M. M., Rauer, C., Süß, D., Griss, P., & Syed Ali, S. (2002). The blood supply of the growth plate and the epiphysis: A comparative scanning electron microscopy and histological experimental study in growing sheep. *Calcified Tissue International*, *70*(4), 312–319. <https://doi.org/10.1007/s00223-001-2006-x>
7. Gibson, J. S., Milner, P. I., White, R., Fairfax, T. P. A., & Wilkins, R. J. (2008). Oxygen and reactive oxygen species in articular cartilage: Modulators of ionic homeostasis. *Pflügers Archiv: European Journal of Physiology*, *455*(4), 563–573. <https://doi.org/10.1007/s00424-007-0310-7>

8. Hollander, J. M., & Zeng, L. (2019). The Emerging Role of Glucose Metabolism in Cartilage Development. *Current Osteoporosis Reports*, 17(2), 59–69. <https://doi.org/10.1007/s11914-019-00506-0>
9. Sautchuk, R., & Eliseev, R. A. (2022). Cell energy metabolism and bone formation. *Bone Reports*, 16, 101594. <https://doi.org/10.1016/j.bonr.2022.101594>
10. Heywood, H. K., Knight, M. M., & Lee, D. A. (2010). Both superficial and deep zone articular chondrocyte subpopulations exhibit the Crabtree effect but have different basal oxygen consumption rates. *Journal of Cellular Physiology*, 223(3), 630–639. <https://doi.org/10.1002/jcp.22061>
11. Zheng, L., Zhang, Z., Sheng, P., & Mobasheri, A. (2021). The role of metabolism in chondrocyte dysfunction and the progression of osteoarthritis. *Ageing Research Reviews*, 66, 101249. <https://doi.org/10.1016/j.arr.2020.101249>
12. Vander Heiden, M. G., Cantley, L. C., & Thompson, C. B. (2009). Understanding the Warburg effect: The metabolic requirements of cell proliferation. *Science (New York, N.Y.)*, 324(5930), 1029–1033. <https://doi.org/10.1126/science.1160809>
13. Hollander, J. M., Li, L., Rawal, M., Wang, S. K., Shu, Y., Zhang, M., Nielsen, H. C., Rosen, C. J., & Zeng, L. (2022). A critical bioenergetic switch is regulated by IGF2 during murine cartilage development. *Communications Biology*, 5(1), 1230. <https://doi.org/10.1038/s42003-022-04156-4>
14. Rajpurohit, R., Mansfield, K., Ohyama, K., Ewert, D., & Shapiro, I. M. (1999). Chondrocyte death is linked to development of a mitochondrial membrane permeability transition in the growth plate. *Journal of Cellular Physiology*, 179(3), 287–296. [https://doi.org/10.1002/\(SICI\)1097-4652\(199906\)179:3<287::AID-JCP6>3.0.CO;2-T](https://doi.org/10.1002/(SICI)1097-4652(199906)179:3<287::AID-JCP6>3.0.CO;2-T)
15. Kan, S., Duan, M., Liu, Y., Wang, C., & Xie, J. (2021). Role of Mitochondria in Physiology of Chondrocytes and Diseases of Osteoarthritis and Rheumatoid Arthritis. *Cartilage*, 13(2_suppl), 1102S-1121S. <https://doi.org/10.1177/19476035211063858>
16. Youle, R. J., & van der Bliek, A. M. (2012). Mitochondrial fission, fusion, and stress. *Science (New York, N.Y.)*, 337(6098), 1062–1065. <https://doi.org/10.1126/science.1219855>

17. Liesa, M., & Shirihai, O. S. (2013). Mitochondrial dynamics in the regulation of nutrient utilization and energy expenditure. *Cell Metabolism*, 17(4), 491–506. <https://doi.org/10.1016/j.cmet.2013.03.002>
18. Rossignol, R., Gilkerson, R., Aggeler, R., Yamagata, K., Remington, S. J., & Capaldi, R. A. (2004). Energy substrate modulates mitochondrial structure and oxidative capacity in cancer cells. *Cancer Research*, 64(3), 985–993. <https://doi.org/10.1158/0008-5472.can-03-1101>
19. Shum, L. C., White, N. S., Mills, B. N., Bentley, K. L. de M., & Eliseev, R. A. (2016). Energy Metabolism in Mesenchymal Stem Cells During Osteogenic Differentiation. *Stem Cells and Development*, 25(2), 114–122. <https://doi.org/10.1089/scd.2015.0193>
20. Forni, M. F., Pelligia, J., Trudeau, K., Shirihai, O., & Kowaltowski, A. J. (2016). Murine Mesenchymal Stem Cell Commitment to Differentiation Is Regulated by Mitochondrial Dynamics. *Stem Cells (Dayton, Ohio)*, 34(3), 743–755. <https://doi.org/10.1002/stem.2248>
21. Moqbel, S. A. A., Zeng, R., Ma, D., Xu, L., Lin, C., He, Y., Ma, C., Xu, K., Ran, J., Jiang, L., & Wu, L. (2022). The effect of mitochondrial fusion on chondrogenic differentiation of cartilage progenitor/stem cells via Notch2 signal pathway. *Stem Cell Research & Therapy*, 13(1), 127. <https://doi.org/10.1186/s13287-022-02758-7>
22. Chen, C.-T., Shih, Y.-R. V., Kuo, T. K., Lee, O. K., & Wei, Y.-H. (2008). Coordinated changes of mitochondrial biogenesis and antioxidant enzymes during osteogenic differentiation of human mesenchymal stem cells. *Stem Cells (Dayton, Ohio)*, 26(4), 960–968. <https://doi.org/10.1634/stemcells.2007-0509>
23. Long, F., & Ornitz, D. M. (2013). Development of the endochondral skeleton. *Cold Spring Harbor Perspectives in Biology*, 5(1), a008334. <https://doi.org/10.1101/cshperspect.a008334>
24. Sophia Fox, A. J., Bedi, A., & Rodeo, S. A. (2009). The basic science of articular cartilage: Structure, composition, and function. *Sports Health*, 1(6), 461–468. <https://doi.org/10.1177/1941738109350438>
25. Shea, C. M., Edgar, C. M., Einhorn, T. A., & Gerstenfeld, L. C. (2003). BMP treatment of C3H10T1/2 mesenchymal stem cells induces both chondrogenesis and osteogenesis. *Journal of Cellular Biochemistry*, 90(6), 1112–1127. <https://doi.org/10.1002/jcb.10734>

26. D'Aniello, C., Cermola, F., Patriarca, E. J., & Minchiotti, G. (2017). Vitamin C in Stem Cell Biology: Impact on Extracellular Matrix Homeostasis and Epigenetics. *Stem Cells International*, 2017, 8936156. <https://doi.org/10.1155/2017/8936156>
27. Shapiro, I. M., & Srinivas, V. (2007). Metabolic consideration of epiphyseal growth: Survival responses in a taxing environment. *Bone*, 40(3), 561–567. <https://doi.org/10.1016/j.bone.2006.09.030>
28. Fujisawa, K., Hara, K., Takami, T., Okada, S., Matsumoto, T., Yamamoto, N., & Sakaida, I. (2018). Evaluation of the effects of ascorbic acid on metabolism of human mesenchymal stem cells. *Stem Cell Research & Therapy*, 9(1), 93. <https://doi.org/10.1186/s13287-018-0825-1>
29. Shukunami, C., Ishizeki, K., Atsumi, T., Ohta, Y., Suzuki, F., & Hiraki, Y. (1997). Cellular hypertrophy and calcification of embryonal carcinoma-derived chondrogenic cell line ATDC5 in vitro. *Journal of Bone and Mineral Research: The Official Journal of the American Society for Bone and Mineral Research*, 12(8), 1174–1188. <https://doi.org/10.1359/jbmr.1997.12.8.1174>
30. Gerstenfeld, L. C., & Landis, W. J. (1991). Gene expression and extracellular matrix ultrastructure of a mineralizing chondrocyte cell culture system. *The Journal of Cell Biology*, 112(3), 501–513. <https://doi.org/10.1083/jcb.112.3.501>
31. Bui, M. D. (2018). *The Effect of Phosphate Deficiency on BMP-2 Treated C3H10T1/2 Mesenchymal Stem Cells* (Order No. 10786571). Available from Dissertations & Theses @ Boston University; ProQuest Dissertations & Theses Global. (2080235416). <https://ezproxy.bu.edu/login?qurl=https%3A%2F%2Fwww.proquest.com%2Fdissertations-theses%2Feffect-phosphate-deficiency-on-bmp-2-treated%2Fdocview%2F2080235416%2Fse-2%3Faccountid%3D9676>
32. Altaf, F. M., Hering, T. M., Kazmi, N. H., Yoo, J. U., & Johnstone, B. (2006). Ascorbate-enhanced chondrogenesis of ATDC5 cells. *European Cells & Materials*, 12, 64–69; discussion 69-70. <https://doi.org/10.22203/ecm.v012a08>
33. Temu, T. M., Wu, K.-Y., Gruppuso, P. A., & Phornphutkul, C. (2010). The mechanism of ascorbic acid-induced differentiation of ATDC5 chondrogenic cells. *American Journal of Physiology. Endocrinology and*

- Metabolism*, 299(2), E325-334.
<https://doi.org/10.1152/ajpendo.00145.2010>
34. Sullivan, T. A., Uschmann, B., Hough, R., & Leboy, P. S. (1994). Ascorbate modulation of chondrocyte gene expression is independent of its role in collagen secretion. *The Journal of Biological Chemistry*, 269(36), 22500–22506.
35. Dawlaty, M. M., Breiling, A., Le, T., Barrasa, M. I., Raddatz, G., Gao, Q., Powell, B. E., Cheng, A. W., Faull, K. F., Lyko, F., & Jaenisch, R. (2014). Loss of Tet Enzymes Compromises Proper Differentiation of Embryonic Stem Cells. *Developmental Cell*, 29(1), 102–111.
<https://doi.org/10.1016/j.devcel.2014.03.003>
36. Murshed, M. (2018). Mechanism of Bone Mineralization. *Cold Spring Harbor Perspectives in Medicine*, 8(12), a031229.
<https://doi.org/10.1101/cshperspect.a031229>
37. Wigner, N. A., Luderer, H. F., Cox, M. K., Sooy, K., Gerstenfeld, L. C., & Demay, M. B. (2010). Acute phosphate restriction leads to impaired fracture healing and resistance to BMP-2. *Journal of Bone and Mineral Research: The Official Journal of the American Society for Bone and Mineral Research*, 25(4), 724–733. <https://doi.org/10.1359/jbmr.091021>
38. Magne, D., Bluteau, G., Faucheux, C., Palmer, G., Vignes-Colombeix, C., Pilet, P., Rouillon, T., Caverzasio, J., Weiss, P., Daculsi, G., & Guicheux, J. (2003). Phosphate is a specific signal for ATDC5 chondrocyte maturation and apoptosis-associated mineralization: Possible implication of apoptosis in the regulation of endochondral ossification. *Journal of Bone and Mineral Research: The Official Journal of the American Society for Bone and Mineral Research*, 18(8), 1430–1442.
<https://doi.org/10.1359/jbmr.2003.18.8.1430>
39. Bottini, M., Mebarek, S., Anderson, K. L., Strzelecka-Kiliszek, A., Bozycki, L., Simão, A. M. S., Bolean, M., Ciancaglini, P., Pikula, J. B., Pikula, S., Magne, D., Volkman, N., Hanein, D., Millán, J. L., & Buchet, R. (2018). Matrix vesicles from chondrocytes and osteoblasts: Their biogenesis, properties, functions and biomimetic models. *Biochimica Et Biophysica Acta. General Subjects*, 1862(3), 532–546.
<https://doi.org/10.1016/j.bbagen.2017.11.005>
40. Kirsch, T., Nah, H. D., Shapiro, I. M., & Pacifici, M. (1997). Regulated production of mineralization-competent matrix vesicles in hypertrophic

chondrocytes. *The Journal of Cell Biology*, 137(5), 1149–1160.
<https://doi.org/10.1083/jcb.137.5.1149>

41. Kirsch, T., Harrison, G., Golub, E. E., & Nah, H. D. (2000). The roles of annexins and types II and X collagen in matrix vesicle-mediated mineralization of growth plate cartilage. *The Journal of Biological Chemistry*, 275(45), 35577–35583.
<https://doi.org/10.1074/jbc.M005648200>
42. Boonrungsiman, S., Gentleman, E., Carzaniga, R., Evans, N. D., McComb, D. W., Porter, A. E., & Stevens, M. M. (2012). The role of intracellular calcium phosphate in osteoblast-mediated bone apatite formation. *Proceedings of the National Academy of Sciences*, 109(35), 14170–14175. <https://doi.org/10.1073/pnas.1208916109>
43. Pei, D.-D., Sun, J.-L., Zhu, C.-H., Tian, F.-C., Jiao, K., Anderson, M. R., Yiu, C., Huang, C., Jin, C.-X., Bergeron, B. E., Chen, J.-H., Tay, F. R., & Niu, L.-N. (2018). Contribution of Mitophagy to Cell-Mediated Mineralization: Revisiting a 50-Year-Old Conundrum. *Advanced Science (Weinheim, Baden-Wuerttemberg, Germany)*, 5(10), 1800873.
<https://doi.org/10.1002/advs.201800873>
44. Roy, R., Kudryashov, V., Binderman, I., & Boskey, A. L. (2010). The role of apoptosis in mineralizing murine versus avian micromass culture systems. *Journal of Cellular Biochemistry*, 111(3), 653–658.
<https://doi.org/10.1002/jcb.22748>
45. Garimella, R., Bi, X., Camacho, N., Sipe, J. B., & Anderson, H. C. (2004). Primary culture of rat growth plate chondrocytes: An in vitro model of growth plate histotype, matrix vesicle biogenesis and mineralization. *Bone*, 34(6), 961–970. <https://doi.org/10.1016/j.bone.2004.02.010>
46. Garrido, C., Galluzzi, L., Brunet, M., Puig, P. E., Didelot, C., & Kroemer, G. (2006). Mechanisms of cytochrome c release from mitochondria. *Cell Death and Differentiation*, 13(9), 1423–1433.
<https://doi.org/10.1038/sj.cdd.4401950>
47. Pucci, B., Adams, C. S., Fertala, J., Snyder, B. C., Mansfield, K. D., Tafani, M., Freeman, T., & Shapiro, I. M. (2007). Development of the terminally differentiated state sensitizes epiphyseal chondrocytes to apoptosis through caspase-3 activation. *Journal of Cellular Physiology*, 210(3), 609–615. <https://doi.org/10.1002/jcp.20857>

48. Maes, M. E., Grosser, J. A., Fehrman, R. L., Schlamp, C. L., & Nickells, R. W. (2019). Completion of BAX recruitment correlates with mitochondrial fission during apoptosis. *Scientific Reports*, 9(1), 16565. <https://doi.org/10.1038/s41598-019-53049-w>
49. Suen, D.-F., Norris, K. L., & Youle, R. J. (2008). Mitochondrial dynamics and apoptosis. *Genes & Development*, 22(12), 1577–1590. <https://doi.org/10.1101/gad.1658508>
50. Youle, R. J., & Karbowski, M. (2005). Mitochondrial fission in apoptosis. *Nature Reviews. Molecular Cell Biology*, 6(8), 657–663. <https://doi.org/10.1038/nrm1697>
51. Karbowski, M., Lee, Y.-J., Gaume, B., Jeong, S.-Y., Frank, S., Nechushtan, A., Santel, A., Fuller, M., Smith, C. L., & Youle, R. J. (2002). Spatial and temporal association of Bax with mitochondrial fission sites, Drp1, and Mfn2 during apoptosis. *The Journal of Cell Biology*, 159(6), 931–938. <https://doi.org/10.1083/jcb.200209124>
52. Arnoult, D., Rismanchi, N., Grodet, A., Roberts, R. G., Seeburg, D. P., Estaquier, J., Sheng, M., & Blackstone, C. (2005). Bax/Bak-dependent release of DDP/TIMM8a promotes Drp1-mediated mitochondrial fission and mitoptosis during programmed cell death. *Current Biology: CB*, 15(23), 2112–2118. <https://doi.org/10.1016/j.cub.2005.10.041>
53. Woods, A., Wang, G., & Beier, F. (2007). Regulation of chondrocyte differentiation by the actin cytoskeleton and adhesive interactions. *Journal of Cellular Physiology*, 213(1), 1–8. <https://doi.org/10.1002/jcp.21110>
54. Zanetti, N. C., & Solursh, M. (1984). Induction of chondrogenesis in limb mesenchymal cultures by disruption of the actin cytoskeleton. *The Journal of Cell Biology*, 99(1 Pt 1), 115–123. <https://doi.org/10.1083/jcb.99.1.115>
55. Lauer, J. C., Selig, M., Hart, M. L., Kurz, B., & Rolauffs, B. (2021). Articular Chondrocyte Phenotype Regulation through the Cytoskeleton and the Signaling Processes That Originate from or Converge on the Cytoskeleton: Towards a Novel Understanding of the Intersection between Actin Dynamics and Chondrogenic Function. *International Journal of Molecular Sciences*, 22(6), 3279. <https://doi.org/10.3390/ijms22063279>
56. Wang, G., & Beier, F. (2005). Rac1/Cdc42 and RhoA GTPases antagonistically regulate chondrocyte proliferation, hypertrophy, and apoptosis. *Journal of Bone and Mineral Research: The Official Journal of*

the American Society for Bone and Mineral Research, 20(6), 1022–1031.
<https://doi.org/10.1359/JBMR.050113>

57. Nurminsky, D., Magee, C., Faverman, L., & Nurminskaya, M. (2007). Regulation of chondrocyte differentiation by actin-severing protein adseverin. *Developmental Biology*, 302(2), 427–437.
<https://doi.org/10.1016/j.ydbio.2006.09.052>
58. Moore, A. S., Wong, Y. C., Simpson, C. L., & Holzbaur, E. L. F. (2016). Dynamic actin cycling through mitochondrial subpopulations locally regulates the fission-fusion balance within mitochondrial networks. *Nature Communications*, 7, 12886. <https://doi.org/10.1038/ncomms12886>
59. Li, S., Xu, S., Roelofs, B. A., Boyman, L., Lederer, W. J., Sesaki, H., & Karbowski, M. (2015). Transient assembly of F-actin on the outer mitochondrial membrane contributes to mitochondrial fission. *The Journal of Cell Biology*, 208(1), 109–123. <https://doi.org/10.1083/jcb.201404050>
60. Sage, D., Donati, L., Soulez, F., Fortun, D., Schmit, G., Seitz, A., Guiet, R., Vonesch, C., & Unser, M. (2017). DeconvolutionLab2: An open-source software for deconvolution microscopy. *Methods (San Diego, Calif.)*, 115, 28–41. <https://doi.org/10.1016/j.ymeth.2016.12.015>
61. Kirshner, H., Aguet, F., Sage, D., & Unser, M. (2013). 3-D PSF fitting for fluorescence microscopy: Implementation and localization application. *Journal of Microscopy*, 249(1), 13–25. <https://doi.org/10.1111/j.1365-2818.2012.03675.x>
62. Chaudhry, A., Shi, R., & Luciani, D. S. (2020). A pipeline for multidimensional confocal analysis of mitochondrial morphology, function, and dynamics in pancreatic β -cells. *American Journal of Physiology. Endocrinology and Metabolism*, 318(2), E87–E101.
<https://doi.org/10.1152/ajpendo.00457.2019>
63. Higaki, T. (2018). Quantitative evaluation of cytoskeletal organizations by microscopic image analysis, *PLANT MORPHOLOGY*, 2017, Volume 29, Issue 1, Pages 15-21, Released on J-STAGE April 06, 2018, Online ISSN 1884-4154, Print ISSN 0918-9726, <https://doi.org/10.5685/plmorphol.29.15>, https://www.jstage.jst.go.jp/article/plmorphol/29/1/29_15/_article/-char/en
64. Manders, E. M. M., Verbeek, F. J., & Aten, J. A. (1993). Measurement of co-localization of objects in dual-colour confocal images. *Journal of*

Microscopy, 169(3), 375–382. <https://doi.org/10.1111/j.1365-2818.1993.tb03313.x>

65. Greenawalt, J. W., Rossi, C. S., & Lehninger, A. L. (1964). EFFECT OF ACTIVE ACCUMULATION OF CALCIUM AND PHOSPHATE IONS ON THE STRUCTURE OF RAT LIVER MITOCHONDRIA. *The Journal of Cell Biology*, 23(1), 21–38. <https://doi.org/10.1083/jcb.23.1.21>

CURRICULUM VITAE

